AEDC-TR-67-201

cy 4

THE COLLECTION OF A NORMALLY INCIDENT LOW DENSITY SUPERSONIC STREAM BY A CRYOGENIC SURFACE

W. B. Stephenson
ARO, Inc.

January 1968

AEROSPACE ENVIRONMENTAL FACILITY
ARNOLD ENGINEERING DEVELOPMENT CENTER
AIR FORCE SYSTEMS COMMAND
ARNOLD AIR FORCE STATION, TENNESSEE

NOTICES

THE COLLECTION OF A NORMALLY INCIDENT LOW DENSITY SUPERSONIC STREAM BY A CRYOGENIC SURFACE

W. B. Stephenson
ARO, Inc.

FOREWORD

The research presented in this report was sponsored by the Arnold Engineering Development Center (AEDC), Air Force Systems Command (AFSC), Arnold Air Force Station, Tennessee, under Program Element 6240533F, Project 8953, Task 895306.

The results presented were obtained by ARO, Inc. (a subsidiary of Sverdrup & Parcel and Associates, Inc.), contract operator of AEDC, under Contract AF 40(600)-1200. The research was conducted from January 1965 to June 1967 under ARO Projects SW2508 and SW5704. The manuscript was submitted for publication on August 30, 1967.

The following acknowledgements are made for direct aid and support in conducting this research: Instrumentation, D. D. Parker; Chamber Operation, D. J. Watson; Shop Work, F. J. Sernicola; Design of Test Equipment, M. J. Triplett and J. T. Rush; and Data Reduction and Analysis, P. Müller.

This technical report has been reviewed and is approved.

Carl E. Simmons Captain, USAF Research Division Directorate of Plans and Technology	Edward R. Feicht Colonel, USAF Director of Plans and Technology

ABSTRACT

An experimental investigation was made to determine the amount of a low density supersonic ($M \equiv 3$) gas stream that will condense on a cryogenic surface at normal incidence. Nitrogen and argon flows up to 2×10^{-3} gm/sec/cm^2 at total temperatures from 300 to 750°K condensed on a liquid- or gaseous-helium-cooled plate. The amount collected was related to the stream properties and the heat transfer to the coolant. The analysis indicates that the cryosurface tends to a steady temperature at which the net rate of collection is the incident stream flux minus the evaporation rate for that temperature. This model provides a basis for the design of cryopumping geometries for low density directed flows such as jet plumes or wind tunnel nozzles.

CONTENTS

APPENDIXES

NOMENCLATURE

A_c	Cryosurface area normal to stream
a	Acoustic speed
C	Specific heat of copper
C_p	Specific heat of gas at constant pressure
e	Thermocouple potential
H_f	Heat of fusion
H_v	Heat of vaporization
h	Heat-transfer coefficient, nondimensional (Defined in Paragraph 5.1.4)
M	Mach No., mass, molecular weight
m_c	Condensed mass
$\dot{m}_c$	Coolant mass flow rate
m_i	Incident flow mass
m_v	Evaporated mass
P	Pressure
$\dot{q}$	Heat flux
R	Gas constant
T	Temperature
t	Time
u	Velocity
V	Volume, molar volume
V_G	Molar volume of gas
V_s	Molar volume of solid
γ	Ratio of specific heats
ρ	Density

SUBSCRIPTS

B	Boiling
c	Cryosurface or coolant

can	Conditions in canister
cool	Coolant
i	Incident
IN	Inlet
OUT	Outlet
o	Initial condition or standard temperature and pressure (STP)
p	Pitot
rad	Radiation
rm	Room conditions (~300°K)
T	Stagnation point condition
T_1	Stagnation point condition ahead of normal shock
T_2	Stagnation point condition behind normal shock
v	Evaporation, vapor
∞	Conditions in undisturbed stream

SECTION I
INTRODUCTION

The purpose of the present investigation was to determine the influence of a cryogenic wall perpendicular to a low density supersonic gas stream. The application to high altitude test facilities for the pumping of directed gas streams from low density nozzles or rocket exhaust fields requires the development of an analytical model and experimental data. Previous experience in cryopumping is based on the random strike rate of a gas several orders of magnitude smaller than treated herein: 10^{16} compared to 5×10^{19} molecules/sec/cm^2. The high flux rate and non-Maxwellian velocity distribution make the application of conventional cryopumping data questionable when applied to directed flow pumping.

The origin of this research was in a development test for a high altitude atmospheric sampling probe reported in Refs. 1 through 4. This probe had liquid-helium (LHe)-cooled vanes that extended to form a disk normal to the flight direction. At the end of the sampling period, the vanes were retracted into the vehicle and the cover sealed. As the vanes warmed, the collected gases evaporated and were retained inside the vehicle for analysis. The effect of cooling the model during test was observed in the behavior of the normal bow shock wave. When the temperature was low, no shock wave stood ahead of the body. As the surface was warmed by the incident gas flow, the shock suddenly appeared close to the surface and then gradually moved out to the usual blunt-body position. This marked alteration in a supersonic flow field suggested a general research program concerning the influence of cryogenic walls. A number of applications to high altitude flight and low density ground test facilities were suggested. Among these, the following are worth investigation: (1) the enhancement of vehicle stability and control effectiveness, (2) the modification of the wake of reentering bodies, (3) the improvement of inlet characteristics, (4) pumping systems for low density wind tunnels, and (5) cryopumping configurations for free-jet expansions in space chambers. The object of this investigation was to investigate the collection of several species of gas by a normally incident surface over a wide range of supersonic stream conditions. References 1 through 4 show the amount of M = 3 air collected by an LHe- or neon (Ne)-cooled surface when the nozzle supply pressure was 148 μ Hg and total temperature was 480°K.

This investigation was planned to cover the operating range of the M = 3 nozzle with supply pressures from 50 to 500μ Hg and total temperatures from 300 to 1000°K. Carbon dioxide, nitrogen, and argon

were to be the test gases. Incident mass flow rates were between 0.2 and 2.0×10^{-3} gm/sec/cm^2, which corresponds to molecular fluxes of from 5×10^{18} to 5×10^{19} molecules/sec/cm^2. This compares to about 10^{16} molecules/cm^2/sec for a high intensity molecular beam apparatus or to a pressure of 10^{-4} mm Hg in the static case. The expansion to a Mach No. of 3 gives stream velocities corresponding to total temperatures of 300 and 1000°K: (1) CO_2 - 700 and 1300 m/sec, (2) N_2 - 700 and 1400 m/sec, and (3) A - 460 and 840 m/sec. It should be noted that the Mach number is not an important similarity parameter for very blunt bodies.

The experimental part of the investigation comprised four entries in the 8V chamber outlined below.

Entry	Dates	Test Gases	Cryosurface Coolant	Cryogenic Equipment
1	December 1965 - February 1966	N_2(1 run) and CO_2	LHe and LN_2	1-kw Refrigerator - 100-ℓ dewar
2	May 1966 - June 1966	N_2 (6 runs)	LHe	1-kw Refrigerator - 500-ℓ dewar
3	January 1967	N_2 and A (27 runs)	LHe and GHe	4-kw Refrigerator - 1000-ℓ dewar
4	April 1967	N_2 and A (16 runs)	GHe	4-kw Refrigerator

The earlier tests (Refs. 1 through 4) required a total temperature of 500°K, whereas the present research was extended to 750°K. The redesigned nozzle plenum proved to be inadequate to provide uniformity of flow of the test section in entries 1 and 2. A modified plenum was used for 3 and 4 although the heating elements were not installed until entry 4. The refrigeration available in entries 1 and 2 was limited to the 1-kw gaseous helium (GHe) refrigerator which had deteriorated to about half its rated performance. Subsequently the 4-kw Mark I chamber refrigerators were connected into the development chamber area, which made it possible to use gaseous helium as a coolant in the test cryosurface.

SECTION II
EXPERIMENTAL APPARATUS

The special test hardware for this investigation was mounted in the 8V chamber (Fig. 1, Appendix I), a stainless steel tank 3.0 m in diameter and 6.1 m long. A Mach No. 3, 10-deg half-angle conical nozzle

with 76-cm exit diameter is located at one end of the chamber (Fig. 2). The nozzle flow is cryopumped by an array of GHe-cooled panels shown at the opposite end. Prior to starting the nozzle flow, the chamber can be pumped to the 10^{-8} torr range with a mechanical roughing pump, a 6-in. diffusion pump, and the cryosurfaces.

Figure 3 shows the M = 3 nozzle, instrumentation, and the test cryosurface installation. The nozzle throat area was surrounded by a LN_2 jacket. Copper cooling tubes were strapped along the conical part of the nozzle and cooled the walls by radiation and imperfect conduction paths. The wall cooling reduced the boundary-layer thickness.

Resistance heating elements were fastened to the plenum liner with spotwelded stainless shim stock strips. Two separate power supplies of 6.7 and 21.7 kw powered the heaters on the end and sides of the plenum. A thermostatic control from two thermocouples provided an on-off regulation. A gas pre-heater made of a coil of Inconel® tubing was operated similarly by a 3-kw power supply.

In order to measure the amount of gas collected on the cryosurface, it was swung outside the stream and enclosed by a canister as shown schematically in Fig. 4. The cryosurface was rotated from the canister position to the axis of the nozzle by a linkage to an external operating lever. The canister was moved axially by a pneumatic cylinder outside the chamber to make a pressure seal with the cryosurface backup plate shown in Fig. 5. With the canister retracted by the cylinder, the cryosurface could be swung to the center of the nozzle. A limit switch operated by the actuating arm prevented the canister from being closed until the cryosurface was in place. A 1.9-cm internally chamfered pitot tube was attached to the cryosurface support arm so that it was on the nozzle axis when the cryosurface was in the canister.

The construction of the 25-cm-diam copper cryosurface is shown in Fig. 6 in two sections. The vapor pressure thermometer bulb is integral with the center stud. The cryosurface was assembled with vacuum-quality inert-gas welding, and the forward surface machined flat. It was then hand polished with fine emery paper.

The cooling system schematic is shown in Fig. 7. The 4-kw Mark I refrigerator supplies a transfer line to the 8V chambers and to other loads. The test cryosurface was supplied by two lines brought to the forward end of the chamber and connected by flexible lines to the movable cryosurface support arm. The bypass valve between the refrigerator outlet and inlet was partially open during cooldown of the system, and its position results in a variation of gaseous helium flow from run to run. A maximum helium flow of 125 gm/sec can be delivered by refrigerators.

During a few runs LHe was supplied from dewars of 500- and 1000-liter capacity filled from the laboratory liquefier. The dewars were located above the chamber, and a transfer line led to a feedthrough. Inside the chamber flexible lines connected to the cryosurface. The exhaust helium was vented to atmosphere through a check valve.

SECTION III
INSTRUMENTATION AND MEASUREMENT ACCURACY

3.1 NOZZLE FLOW

The characteristics of the nozzle flow depend upon the supply pressure, P_{T1}, the pitot pressure (P_p), the total temperature (T_T), the nozzle wall temperature, and, to a minor extent, upon the chamber pressure. The range of pressures, P_p and P_{T_1}, is from 20 to 500 μ Hg. Two instruments were used: (1) the Alphatron® radium source ionization gage with ranges from 10^{-4} to 1000 mm Hg, and (2) the Baratron® differential pressure transducer with a maximum range of 3 mm Hg. The latter was used as an absolute pressure gage by connecting one side to a reference system pumped by a 2-in. diffusion pump which maintained a pressure in the 10^{-5} to 10^{-6} mm Hg range. There is considerable difficulty in determining the absolute accuracy of these gages because the secondary standards available for calibration (McLeod gages) are quoted as ±6 μ Hg from 0 to 200 μ Hg and ±20 μ Hg from 200 to 500 μ Hg. On the other hand, the Baratron manufacturer gives 0.05 percent accuracy, which is about the same as the ±0.1 μ Hg reading resolution. The Alphatron reading resolution is about ±1 percent full scale, and this is also less than that of the secondary standard. A direct comparison of the two instruments showed that they were within the 1 percent full-scale reading of each other. More precise evaluation of absolute accuracy was not practicable.

An Alphatron measured the plenum pressure and a Baratron was connected to the pitot tube. Another Alphatron was mounted on the nozzle wall primarily to give an indication of flow breakdown, which will result from excessive chamber pressure.

The chamber pressure was measured with an Alphatron and a Bayard-Alpert ion gage in the low range prior to starting the nozzle flow.

The total temperature (from 300 to 1000°K) was measured at eight points on the plenum wall between heating elements by Chromel®-Alumel® thermocouples. These were held in place with strips of Inconel shim

stock spotwelded to the outside of the cylindrical shell and end plate. One of the five thermocouples on the cylinder operated the controller for the plenum side wall heater power supply. One of the three end thermocouples controlled the plenum end heater power. A similar controller operated the gas inbleed heater.

There were two copper-constantan thermocouples at the nozzle throat and two at each of two stations on the conical part. The throat section varied from 90 to 140°K and the cone from 110 to 170°K depending on time after the start of cooling and nozzle flow condition.

3.2 CRYOSURFACE TEMPERATURE MEASUREMENT

For these experiments a record of cryosurface temperature versus time was desired. The transient temperature measurement was made with three Chromel-constantan thermocouple junctions soft-soldered to the face of the cryosurface and referenced to a liquid nitrogen bath. The bath temperature was measured with a platinum resistance thermometer calibrated to about 0.01°K. About one meter of the thermocouple leads was wrapped around the coolant inlet line for tempering.

To obtain steady-state temperatures of the cryosurface and to provide an in-place calibration of the thermocouples, a hydrogen vapor pressure thermometer bulb was made integral with the cryosurface. A 0- to 300-psia pressure gage measured the hydrogen pressure, which was about 7 atm at room temperature. The pressure gages were calibrated against a 0- to 800-mm Hg aneroid-type gage for the low pressure end of their scales. The temperature could then be determined to ±0.05°K near 20°K.

3.3 CANISTER PRESSURE AND TEMPERATURE

The canister pressure was measured by a 0- to 800-mm Hg aneroid gage calibrated to give a resolution of about 0.5 mm Hg. It was located outside the chamber and connected with a 5-cm-diam flexible line to the canister.

The temperature of the canister was determined from the output of four copper-constantan thermocouples spotwelded to the outside in four places. They were read out on a multipoint thermocouple chart recorder.

3.4 CRYOSURFACE POSITION

A potentiometer was attached to the cryosurface operating lever shaft to indicate its position. A mercury cell across the total resistance provided the potential. The output was put on a strip chart recorder running at 2 in. /min for a resolution of about 0.5 sec of time.

3.5 ACCURACY OF MEASUREMENTS

In summary the quantities that constitute the experimental data are (1) the incident stream mass flux, (2) gas collected by the cryosurface, and (3) the cryosurface temperature history. The stream flow depends upon pitot pressure corrected for viscous effect at low density, the Mach number which is determined by the ratio of stagnation pressure to supply pressure (P_{T_2}/P_{T_1}), and the total temperature. If the pitot pressure is used for setting the test conditions, as it was in the last two chamber entries, the Mach number and temperature are of secondary importance in determining the mass flux. The stagnation pressure behind the normal shock (P_{T_2}) is directly proportional to mass flux, and errors arise from the uncertainty in the pitot viscous effect and pitot pressure measurement. At a supply pressure of 50 μ Hg the viscous correction may be ±10 percent in error, and at 200 μ Hg it is negligible. The uncertainty in mass flux on the nozzle centerline would then vary from about ±15 percent at a supply pressure of 50 μ Hg and from 1 to 2 percent above 200 μ Hg.

The total incident mass depends upon the time in the flow, and this is related to the speed at which the cryosurface was moved and the nozzle boundary layer. Examination of the swing-arm position traces shows that the time required to move the cryosurface from the canister to the nozzle centerline, or the reverse, was approximately a second. The time that the cryosurface was within the nozzle flow was therefore known to 0.5 sec or better. The shortest run times were about 10 sec, and therefore an error of ±5 percent may be possible for these runs.

The effect of boundary-layer retardation on the mass flux was investigated for the extreme case of the merged layer, which fills the nozzle. One calculates (Ref. 5) that the incident flux will be reduced 10 percent for this case, which corresponds to lower supply pressures than were used. Probably a systematic reduction of from 0 to 3 percent is realistic for the lowest pressure levels.

The gas collected by condensation on the cryosurface is determined by measurement of the canister system pressure and the canister temperature after the surface warms. The pressure was accurate to about

±0.5 mm Hg out of from 75 to 800 mm Hg; therefore, the collected mass may be from ±0.1 to ±0.7 percent in error from this source. The temperatures measured by thermocouples on the canister are estimated as ±5°K out of 250°K or 2 percent. Therefore, the mass collected may be from 0 to ±3 percent in error at the low mass collected.

SECTION IV
EXPERIMENTAL RESULTS

4.1 NOZZLE CALIBRATIONS

The calibration of the 76-cm-diam M = 3 nozzle included horizontal profiles measured with a 1.9-cm pitot tube 2 cm downstream of the exit plane. Figures 8 and 9 show typical profiles for nitrogen and argon. Between the supply pressure limits of from 50 to 500 μ Hg, these are sufficiently flat that the stream mass flux is essentially uniform over the cryosurface. The LN_2-cooled nozzle wall temperature was between 110 and 170°K, and the throat between 90 and 140°K. The nozzle and throat were not cooled during the carbon dioxide tests because the excessive condensation of the test gas resulted in a large and variable expansion ratio (or Mach number). The symmetry of the CO_2 profiles is rather poor at supply pressures greater than about 100 μ Hg.

The centerline calibration of the nozzle requires an estimate of the pitot tube viscous correction at the low end of the supply pressure range. The best available data (Ref. 6) are shown in Fig. 10 for internally chamfered pitot tubes. These have an undesirably large spread, and the mean curve shown was used in the pitot data reduction. Figures 11 and 12 show the measured pitot pressure, the Rayleigh stagnation pressure (p_{T_2}), and the Mach number calculated from the ratio p_{T_2}/p_{T_1}. These curves are terminated at the point where the boundary layer appears to merge, and the centerline flow is no longer isentropic at lower supply pressures.

Figure 13 provides more insight into the stream conditions by showing the ranges for Reynolds number and mean free path.

For the present experiments, the most important stream property is the mass flux through the nozzle exit region where the cryosurface is located. The incident mass flow at the cryosurface,

$$\dot{m}_i = \rho_\infty u_\infty A_c$$

can be expressed in terms of Mach number and gas properties as

$$\frac{m_1\sqrt{T_T}}{A_c} = \sqrt{\frac{\gamma}{R}}\left[\frac{P_{T_1}}{P_{T_2}}\ \frac{\rho_\infty}{\rho_{T_1}}\ \frac{u_\infty}{a_T}\right]P_{T_2}$$

$$= \left[f(\gamma, R, M)\right]P_{T_2}$$

This relation, shown in Fig. 14, can be seen to be relatively insensitive to Mach number of the stream at Mach number variations associated with nozzle calibration. The major difficulties associated with repeatability of nozzle calibration are circumvented by setting the test conditions with a pitot tube, and this was the procedure used during the cryopumping runs. Figure 15 shows the mass flux for nitrogen and argon over the available total temperature range from 300 to 750°K. Figure 16 gives the Mach number and mass flow for carbon dioxide in the nozzle at 300°K total temperature.

The plenum wall temperatures, assumed equal to the total temperatures, were measured by Chromel-Alumel thermocouples at eight points. The range of readings is given below for the two nominal temperatures:

T_T = 500 °K	$489 < T_{Meas} < 509$°K	T_{avg} = 495°K
T_T = 750°K	$736 < T_{Meas} < 773$	T_{avg} = 749°K

The average plenum wall temperatures are within one percent of the nominal, and, therefore, the stream mass flux ($\sim 1/\sqrt{T_T}$) would be within one-half percent.

4.2 GAS COLLECTION MEASUREMENTS

The procedure followed during the condensation experiments was the following:

1. The cryosurface in the canister was cooled to the minimum available temperature as indicated by the hydrogen vapor pressure thermometers.
2. The nozzle conditions were set: (a) total temperature indicated by the plenum thermocouples, (b) pitot pressure from the tube on the swing arm.
3. The canister was opened, the cryosurface was swung into the center of the nozzle, and returned to the canister, which was then closed.

4. The cryosurface coolant flow was valved off and the canister pressure was read until it became constant.

The time in the flow was determined from a strip chart readout of the swing-arm position potentiometer to a resolution of ±0.5 sec. Both the times at which the center of the cryosurface reached the edge of the nozzle and the time when the edge of the cryosurface was tangent to the nozzle edge were used to specify the time interval. The difference between these time intervals was less than a second. It is reasonable to assume that the time is known to ±0.5 sec and therefore the incident mass on the surface is ±0.1 gm at the low flow rate to about ±0.5 gm at the maximum rate.

The amount of gas collected by the cryosurface was determined by the volume, pressure, and temperature in the canister system.

$$m_c = \frac{P_{can}}{R}\left(\frac{V_{can}}{T_{can}} - \frac{V_{gage + tube}}{T_{rm}}\right)$$

where the canister temperature (T_{can}) is taken as the average of the four thermocouples around the canister. The gage and connecting tubing are assumed to be at room temperature. The canister volume is 10.75 liters and the remaining volume 4.33 liters, of which 3.07 liters is in the gage. There is some uncertainty in the temperature of the gas in the canister because the cryosurface temperature remains lower than the canister walls. However, a check made by leaving the canister closed overnight to permit the temperatures to equalize indicated the same mass collected. The uncertainty in the measurement of temperature and pressure in the canister is considered negligible. However, a more important source of error occurred in 11 of the 16 runs of the April series. This was leakage of the canister seal probably as a result of low temperature of the backup plate freezing the O-ring seal. Figure 17 shows the pressure-time variation for the worst of these runs. The corrected pressure, based on the linear leak after the maximum, is about 10 percent higher than the measured maximum. This is about 1.6 gm of gas out of the 16 collected. Of the remaining ten runs, one had a correction of 5 percent, one 3 percent, and the rest were less than 2 percent.

In Figs. 18a and b the mass of gas (nitrogen and argon) collected is plotted against the incident mass derived from the pitot pressure and time in the flow. Figure 18a shows the data for a total temperature near 300°K with the cryosurface cooled by liquid helium (LHe) and gaseous helium (GHe) from a refrigerator. The amount of gas collected by LHe and GHe cooling was about the same at low incident fluxes; however, the

LHe was inferior at large incident mass. This suggests that the low initial temperature of the LHe cooling was not superior and that the liquid coolant flow rate was limited. The heat removal rate by the coolant appears to be insufficient to maintain the temperature low enough for continued condensation.

Figure 18b shows the influence of raising the total temperature on the amount of gas collected. Several points are noted in Fig. 18:

1. At low mass and heat fluxes, the amount of gas collected is equal to the incident mass.
2. At higher fluxes, as the total incident mass is increased the collected mass is initially equal and then approaches a constant slope less than unity.
3. The collection ratio for argon is consistently higher than for nitrogen at the same condensation heat flux.

One can infer a model of the capture process based on total condensation as the temperature rises to an equilibrium level. At this point the incident heat is equal to the heat removed by the coolant, and a steady evaporation rate is established. The vapor pressure of argon is only 5 percent of that of nitrogen at 40°K, which lends more weight to the hypothesis. Correlations based on this model are given in Section V.

There appears to be a lower collection rate in the data of Ref. 1 shown in Fig. 18b. However, there may be a systematic error resulting from the fact that the incident mass was derived from visual observation of the time in the flow measured with a stop watch. These data have been corrected for the new nozzle calibration. The Mach number is close to 3. 0 compared to 2. 8 quoted in the reference.

The data of Fig. 19 were taken in the first test entry for the collection of CO_2 nozzle flow at room temperature. Liquid nitrogen from the laboratory supply system was the coolant. In this series, the nozzle calibration was relied on to provide the incident mass flux rather than a pitot tube reading immediately before the cryosurface was swung into the flow. This accounts for the large uncertainty in incident mass. Within the accuracy of the measurements, it appears that all the incident flow was condensed.

During the test program reported in Ref. 1 porous disks (made of perforated sheet) were run in place of the cryosurface, and the shock detachment distance was observed photographically. In Appendix II of this report, a correlation of detachment distance showed that the disappearance of the shock in front of a blunt body would correspond to a

condensation fraction greater than 90 percent. This number is consistent with the mass collection fractions measured during this test. Reference 1 indicates that the fraction should be about 80 percent, which is apparently too low.

4.3 TEMPERATURE MEASUREMENTS

4.3.1 Cooldown of Cryosurface

No reliable cryosurface temperature could be measured when liquid helium was the coolant. The hydrogen vapor pressure gages were not sufficiently accurate at these temperatures, and the three surface thermocouples indicated from 5 to 25°K at the same time. Three typical cooldowns with gaseous helium are illustrated in Fig. 20, which shows the inlet, outlet, and cryosurface temperatures indicated by the hydrogen vapor pressure thermometers. These appear to be in reasonable agreement at about a 17°K inlet and approximately a one-degree temperature rise. The cryosurface is about 0.5 deg higher than the outlet temperature. The surface thermocouples, which should indicate the same as the cryosurface hydrogen vapor pressure thermometer, are from 6 deg lower to 10 deg higher. There was a large zero suppression because the reference junctions are in liquid nitrogen. It is impossible to determine whether the discrepancies are the result of different sensitivities of the individual junctions or electrical zero shift.

4.3.2 Temperatures during Cryopumping run

Figure 21 shows transient temperatures indicated by the thermocouples during several typical runs. The temperatures were shifted to coincide with the initial hydrogen vapor pressure thermometer indication. Figure 21b shows that the absolute temperature is not reliable; the three runs were made at the same incident conditions and show wide differences whether or not the correction is applied.

A further peculiarity noted in Fig. 21 is the trend of the temperatures downward after a maximum. It is not possible to say whether this is a real effect or a characteristic of the instrumentation. It is conceivable that the heat-transfer coefficient may increase with surface temperature and a decrease in temperature occur.

4.3.3 Temperature Rise in Canister

In order to find the heat-transfer rate to the coolant, the temperature-time variation was required when the cryosurface was in the canister and the coolant flow shut off. Figure 22 is a trace of a typical strip chart record of the surface thermocouple output with time. The signal is very

nearly linear for from 30 to 60 sec. It is extended to the level before the run at which point the actual temperature is known from the hydrogen vapor pressure. This temperature was usually different from the thermocouple calibration.

In summary, accurate temperature measurements were possible only under static conditions through use of the hydrogen vapor pressure thermometers. The cryosurface thermocouples (Chromel-constantan) provided the only transient measurements, but their indications were in error from 5 to 10°K high or low.

SECTION V
ANALYSIS

When gaseous helium is used to cool the cryosurface, the experimental results show a capture fraction of approximately unity for low incident mass fluxes and initially for higher fluxes. At the higher flows and temperatures, the capture fraction appears to reach a steady value less than one. The surface temperature, measured by thermocouples, showed a transient of about 10 sec followed by a leveling off which suggests an equilibrium between the incident heat rate and the coolant heat removal. A simple model of this behavior is suggested: (1) all the incident gas flux condenses on the cryosurface, (2) the rate of evaporation is determined by the surface temperature, and (3) the surface temperature history results from the thermal balance of incident flow sensible heat and heat of condensation, the radiation to the surface, the heat of vaporization of the evaporating gas, and the heat transferred to the coolant.

The verification of the above model would be simple if an accurate temperature-time history of the cryosurface could be measured during the run. However, instrumentation with the required accuracy (±1°K) combined with adequate time response was not available for this experiment. Therefore, it was necessary to attempt to calculate the temperature variation from limited experimental data. These were: (a) the steady-state temperature of the cryosurface at the end of cooldown before the run, (b) the gaseous helium coolant inlet and outlet temperatures at the same time and (c) the temperature rise rate of the cryosurface after the coolant flow was shut off.

5.1 CRYOSURFACE TEMPERATURE EQUATION

The high thermal conductivity of copper, particularly at low temperature (Ref. 7), allows the assumption of uniform temperature. The heat balance equation can be written for the cryosurface mass, M, with specific heat, $C(T_C)$:

$$M \cdot C(T_c) \cdot \frac{dT_c}{dt} = \dot{q}_i + \dot{q}_{rad} - \dot{q}_v - \dot{q}_{cool}$$

where

$\dot{q}_i = \dot{m}_i \left[C_{p_i}(T_T - T_c) - H_v\right]$ — incident gas

$\dot{q}_{rad}$ corresponds to radiation from surroundings

$\dot{q}_v = \dot{m}_v \cdot H_v$ — evaporating gas

$\dot{q}_{cool}$ corresponds to heat removed by the coolant

$\dot{m}_i$ is the incident mass flux through a stream cross section whose area is the same as the cryosurface. The heat of vaporization and condensation, H_V, the evaporating mass flux, $\dot{m}_V$, and the specific heat of the cryosurface are functions of the temperature T_C.

5.1.1 $\dot{m}_v$

The mass rate of evaporation is calculated directly from the vapor pressure (Ref. 8):

$$\dot{m}_V = \frac{\sqrt{M}}{17.14} \frac{P_v}{\sqrt{T_v}} A_c$$

where

M = molecular wt

P_v = vapor pressure (mm Hg)

T_v = temperature (°K) = T_C

A_c = cryosurface area (cm^2)

See Fig. 23.

Then the amount of gas captured on the cryosurface is

$$m_c = m_i - m_v = m_i - \int_0^t \dot{m}_v \, dt$$

The heat of vaporization and condensation, H_V, is computed for various temperatures from the vapor pressure data (Ref. 9):

$$H_v = \text{Constant} + H_f + RT \ln (V_G/V_s)$$

where H_f is the heat of fusion and V_G and V_s are the gas and solid molar volumes. This is plotted in Fig. 24 for the three stream gases.

5.1.2 $C(T_c)$

The specific heat of the copper cryosurface as a function of temperature is plotted in Fig. 25 (Ref. 7). The fourth-order polynomial curve fit was developed for use in the computer solutions.

5.1.3 $\dot{q}_{rad}$

The radiant heat load to the cryosurface, $\dot{q}_{rad}$, is small in the experimental geometry because of the large solid angle of the LN_2-cooled nozzle as viewed from the cryosurface. The view factor from the cryosurface to the throat of the nozzle, which is considered as a blackbody at the plenum total temperature, is only 8×10^{-3}. The radiation load varies from about 0.5 to 3.7 cal/sec with total temperature from 300 to 1000°K.

5.1.4 $\dot{q}_{cool}$

The estimation of the heat carried away by the GHe coolant requires knowing the coolant flow rate, $\dot{m}_c$, and a heat-transfer coefficient, h, between the cryosurface and the coolant. These quantities must be arrived at indirectly through measurements of the gas inlet and outlet temperatures and the cryosurface temperature, under steady conditions. In defining the heat-transfer coefficient, the mean coolant temperature, $\bar{T}$, is taken as the average between the inlet and outlet temperatures: $(T_{IN} + T_{OUT})/2$. Then the cooling is given by

$$\dot{q}_{cool} = \dot{m}_c C_{p_c} h (T_c - \bar{T})$$

Under steady heat flow conditions, the assumption of constant h and inlet temperature gives a relation between the temperature differences and h:

$$\dot{m}_c C_{p_c} (T_{OUT} - T_{IN}) = \dot{m}_c C_{p_c} h (T_c - \bar{T})$$

$$h = \frac{(T_{OUT} - T_{IN})_o}{T_{c_o} - \bar{T}_o}$$

where the "o" subscript indicates the minimum temperatures reached during cooling, out of the stream (in the canister). By the elimination

of T_{IN} and T_{OUT}, the mean coolant temperature can be expressed in terms of the cryosurface temperature, T_C:

$$\overline{T} = \frac{h}{2+h} T_c + \overline{T}_o - \frac{h}{2+h} T_{c_o}$$

which provides the coolant heat rate:

$$\dot{q}_{cool} = \dot{m}_c C_{p_c} h (T_c - \overline{T}) = \dot{m}_c C_{p_c} h \left[\left(\frac{2}{2+h}\right) T_c + \left(\frac{h}{2+h}\right) T_{c_o} - \overline{T}_o\right]$$

In summarizing the heat balance the parameter ($\dot{m}\ C_{p_c} h$) is left explicit:

$$M\,C(T_c)\frac{dT_c}{dt} = \dot{m}_i C_{p_i} T_T + q_{rad} - \dot{m}_c C_{p_c} h \left[\left(\frac{h}{2+h}\right) T_{c_o} - \overline{T}_o\right]$$

$$- \left[\dot{m}_i C_{p_i} + \dot{m}_c C_{p_c} h \left(\frac{2}{2+h}\right)\right] T_c + H_v (\dot{m}_i - m_v)$$

$$= K_1 - K_2 T_c + H_v (\dot{m}_i - \dot{m}_v)$$

where

$$K_1 = \dot{m}_i C_{p_i} T_T + \dot{q}_{rad} - \dot{m}_c C_{p_c} h \left(\frac{h}{2+h} T_{c_o} - \overline{T}_o\right)$$

$$K_2 = \dot{m}_i C_{p_i} + \dot{m}_c C_{p_c} h \left(\frac{2}{2-h}\right)$$

Since $h < 1$ and T_{c_O} is not more than 1°K higher than $\overline{T}_O$, K_1 can be simplified to

$$K_1 = \dot{m}_i C_{p_i} T_{\overline{T}} + \dot{q}_{rad} + \dot{m}_c C_{p_c} h \left(\frac{2}{2+h}\right) \overline{T}_o$$

The coolant terms appear in the same form in both K_1 and K_2. A computer program was written to solve the differential equation above in order to calculate the cryosurface temperature variation with time in the stream.

The refrigerator which supplied gaseous helium to the cryosurface also served the cryopump in the chamber and sometimes other facilities. Only a small and unknown fraction of the total refrigerator flow is diverted through the cryosurface. In addition, the temperature of the gas supplied decreases during the period of testing as a result of a continuous cooling of the refrigerator and transfer lines. Therefore, it is necessary to calculate each experimental run individually with generally a different coolant mass flux, $\dot{m}_C$. To find the coolant flow parameter

$\dot{m}_c C_{p_c} h$, it is necessary to know the heat transfer to the cryosurface during cooldown, since

$$\dot{m}_c C_{p_c} h = \frac{\dot{q}_{can}}{T_{c_0} - \bar{T}_0}$$

5.2 HEAT TRANSFER TO CRYOSURFACE DURING COOLDOWN

The rate of rise of temperature when the coolant flow is valved off is proportional to the heat flux, $\dot{q}_{can}$

$$\dot{q}_{can} = M\,C(T_c)\,\frac{dT_c}{dt}$$

in which the derivative should be taken at the minimum temperature because of the rapid change in specific heat with temperature. The transient temperature-time variation was determined by the thermocouple output recorded. However, the absolute temperatures from the thermocouples differed by ±10°K from the hydrogen vapor pressure temperatures, which are considered accurate to ±0.05°K. As discussed in Section 3.2, the sensitivity or zero shift in thermocouple readings can result in large errors. Therefore, the following procedure was used to circumvent the difficulties. In the preceding formula C was taken for the temperature given by the vapor pressure thermometer and

$$dT_c/dt = \left(\frac{de}{dt}\right) / \left(\frac{de}{dT}\right)$$

where de/dT was taken at the thermocouple output, e. A typical thermocouple trace from the recorder is shown in Fig. 22. The temperature corresponding to the output is the abscissa in Fig. 26 where the apparent $\dot{q}_{can}$ is shown. The averages for the two sets of data are close to 1.6 cal/sec, and the mean temperature is close to the vapor pressure thermometer readings. This is actually a method for empirically correcting the thermocouple data for zero shift and sensitivity. An estimate of the radiative heat load from 250 to 300°K canister walls is from 6 to 14 cal/sec for emissivities and absorptivities of one. This is consistent with the observed heat rate.

5.3 HEAT-TRANSFER COEFFICIENT

The heat-transfer coefficient between the cryosurface and coolant was derived as the ratio of the two temperature differences

$$h = \frac{(T_{OUT} - T_{IN})_0}{T_{c_0} - \bar{T}_0}$$

These differences are plotted in Fig. 27 for the two test periods. The slopes of mean curves are h, and these show an unexpected shift between the two sets. The first three runs (5, 6, and 7) of the second set are in line with the first set of data, then runs 8 through 16 seem to form a distinct group around a coefficient h = 1.0. The factor appears in the equation for the cryosurface temperature history in the form 2/(2 + h), so that the factor is 0.8 and 0.67 for the two values of h of 0.5 and 1.0.

5.4 RESULTS OF COMPUTATIONS

Initially the data of the 300°K runs were calculated by using the observed temperature difference between cryosurface and coolant ($T_{c_o} - \overline{T}_o$) at the end of the cooldown to find the cooling parameter, $\dot{m}_c C_{p_c} h$. The heat load to the cryosurface in the canister $\dot{q}_{can}$ was taken to be 1.6 cal/sec. The temperature history equation

$$M\,C(T_c)\frac{dT_c}{dt} = K_1 - K_2 T_c + H_v(\dot{m}_i - \dot{m}_v)$$

contains the constants

$$K_1 = \dot{m}_i C_{p_1} T_T + \dot{q}_{rad} + \dot{m}_c C_{p_c} h\left(\frac{2}{2+h}\right)\overline{T}_o$$

and

$$K_2 = \dot{m}_i C_{p_1} + \dot{m}_c C_{p_c} h\left(\frac{2}{2+h}\right)$$

The term 2/(2 + h) is relatively insensitive to the value of h between 0.5 to 1.0. The coolant parameter term dominates K_2 and is approximately equal to the other terms in K_1. The parameter

$$\dot{m}_c C_{p_c} h = \frac{\dot{q}_{can}}{T_{c_o} - \overline{T}_c} = \frac{1.6}{T_{c_o} - \overline{T}_o}$$

consistently gave a too high surface temperature, i.e., the cooling effect was low. It appeared that there was a systematic error in $\dot{q}_{can}$ (Fig. 26) because when it was arbitrarily assumed to be 2.8 cal/sec, the calculated and observed collected mass agreed within the experimental spread (~ ±1 gm). A typical family of solutions is shown in Fig. 28 for nitrogen at an incident rate of 0.865 gm/sec at 300°K total temperature.

During the second series of runs a peculiar situation developed which is illustrated in Fig. 27. The temperature differences between the cryosurface and coolant decreased by a factor of two, but the inlet-outlet temperature difference remained within the same range as the previous data. This apparent increase in the cooling parameter was

not substantiated by a comparison of the calculated with the experimental mass collected. The calculated amount of cooling resulted in no appreciable re-evaporation of the cryodeposit. This development effectively blocked the deductive approach previously used, and left open only the process of inferring the cooling parameter from a comparison of experimental results with the computer solutions.

For each experimental condition, two or more computer calculations were made with a systematic variation in the coefficients K_1 and K_2. The difference between the observed mass collected and the computed value was plotted against K_2 to find the value for zero difference. The general shape of the curves is indicated in Fig. 29. Then the cooling parameter is given by

$$\left[\dot{m}_c C_{p_c} h\right]\left(\frac{2}{2+h}\right) = K_2 - \dot{m}_1 C_{p_1} \quad \text{at } \Delta m = 0$$

A range of ±1 gm from the intercept shows a realistic experimental scatter in the collected mass measurement. In runs where the incident mass flow is small, only a lower limit in K_2 can be determined since practically all the incident mass was collected. These results are plotted in Fig. 30 as a function of the temperature difference $T_{c_o} - \overline{T}_o$, which should be the appropriate criterion consistent with the preceding analysis. Although this method is somewhat unsatisfactory inasmuch as the two unknown cooling quantities, $\dot{m}_c$ and h, cannot be separated, at least limits can be defined.

The cooling parameter,

$$\left[\dot{m}_c C_{p_c} h\right] \frac{2}{2+h} = \frac{\dot{q}_{can}}{T_{c_o} - \overline{T}_o}\left(\frac{2}{2+h}\right) = \frac{\text{constant}}{T_{c_o} - \overline{T}_o}$$

should be a hyperbola. The constant, $\dot{q}_{can}\left(\frac{2}{2+h}\right)$, in the range from 1 to 2.4 would cover the experimental results. The table below shows values of $\dot{q}_{can}$ and h that correspond to the curve parameters.

$\dot{q}_{can}$, cal/sec	h	$\dot{q}_{can}\left(\frac{2}{2+h}\right)$, cal/sec
1.6 (6.7w)	0	1.6
↓	0.5	1.28
	1.0	1.07
2.8 (11.7w)	0	2.8
↓	0.5	2.24
	1.0	1.87
	2.0	1.40

The two groups of temperature difference data in Fig. 26 fall into the two sets in Fig. 30, which are higher or lower than $T_{co} - \bar{T}_o = 0.5°K$. It can be seen that a $\dot{q}_{can}$ of 2.8 cal/sec and a heat-transfer coefficient, h, of 0.5 would result in a calculated collected mass close to what was measured for the January 1967 set of runs. However, the shift observed during the April 1967 set would require that the heat transfer in cooldown, $\dot{q}_{can}$, drop to about 1.6 cal/sec or that the heat-transfer coefficient, h, change from 0.5 to 2.0. The third possibility is that the temperature differences in the second group of runs are measured about 0.3°K too low as a result of some unknown systematic shift in either the cryosurface temperature, T_{co}, or the mean coolant temperature, $\bar{T}_o$. In summary, it must be concluded that the heat load to the cryosurface during cooldown in the canister is between 1.5 and 3.0 cal/sec (from 6 to 13 w). The heat-transfer coefficient is probably between 0.5 and 1.0. For $1 < \left[\dot{m}_c \, C_{p_c} h\right]\left(\frac{2}{2 + h}\right) < 5$, the range of gaseous helium mass flows, $\dot{m}_c$, is therefore between 1 and 10 gm/sec, which is reasonable when compared with from 60 to 125 gm/sec total supplied by the 4-kw refrigerators. When the cryosurface is in the stream, its temperature rises to an equilibrium level and the coolant carries away the incident condensation heat. For example, the nitrogen stream at 750°K total temperature and a flow of 1 gm/sec will result in about 250 cal/sec or 1 kw. This is consistent with a gaseous helium flow rate of 8 gm/sec and a typical temperature rise from 16°K inlet to 40°K outlet.

An event occurred sometime during the second test series that may have resulted in some change in the cryosurface characteristics. The canister was closed on the edge of the cryosurface, bending its support tubes so that it took a permanent set at about 10-deg permanent deflection. This caused no apparent leakage in the cryogenic lines or the hydrogen vapor pressure thermometer lines which would be immediately observed. It is not anticipated that the external stream flow would be affected since blunt body flows are insensitive to small angles of incidence. There remains the possibility that the internal flow of the coolant may have been altered by the distortion so that the heat-transfer coefficient was increased. The apparent heat-transfer coefficient changed from 0.5 to 1.0 after the first seven runs of the second series. Time was not available to repair the cryosurface during the test period.

5.5 LIQUID COOLANTS

Liquid helium has been used in condensing a 300°K nitrogen stream and liquid nitrogen to condense carbon dioxide. The two-phase nature of

the coolant and lack of reliable data for the boiling heat-transfer characteristics make detailed calculations of the cryosurface temperature impracticable. Figure 31 is an example of the boiling heat transfer from a cylindrical heater to a bath of liquid nitrogen. The surface geometry and orientation to the vertical will have some unknown effects. To complicate the analysis further, the temperature differences observed during the CO_2 tests fell in the metastable boiling range. It was found impossible to obtain solutions for the liquid coolant cases. The runs for a liquid-helium-cooled surface condensing the nitrogen stream showed that the gas collected on the cryosurface was less than for gaseous helium cooling at the long run times. This is the result of (1) a low heat of vaporization, about 5 cal/gm, (2) a low flow rate of liquid, and (3) the small specific heat of the copper cryosurface which permits a rapid initial temperature rise. Difficulties in obtaining liquid helium limited the number of experiments, and it was used only during the 300°K total temperature runs with nitrogen.

SECTION VI
CONCLUSIONS

The collection of a supersonic gas stream on a cryogenic-fluid-cooled surface normal to the flow has been investigated. The analysis shows that within the accuracy of the experimental results a simple model describes the behavior of a supersonic low density gas stream incident upon a normal cold surface.

For incident mass flux rates up to 2×10^{-3} gm/sec/cm^2 and total temperatures to 750°K, the net amount of gas collected is determined by the cryosurface temperature history which results from the balance between the incoming heat and the coolant heat removal. The rate of evaporation is based on the vapor pressure at the cryosurface temperature. A computation program has been developed that may be used to determine the temperature history and net condensation for pumping surfaces at high incidence.

An attempt was made to calculate the cryosurface temperature history during the time in the stream in order to verify this model. Since the heat-transfer properties of the cryosurface coolant could not be determined unambiguously, it can only be concluded that the experimental results were not in conflict with the assumed model.

The application to the design of a pumping configuration for jet plume flow requires knowledge of the spatial distribution of the mass

flux - for instance, characteristics method calculations (Ref. 12). The cryogenic system will determine the heat that can be transferred from the surface. With this information the arrangement of the cryosurfaces can be selected for steady collection or transient operation.

The technique employed in this investigation could be extended to the evaluation of more complex cryopumping arrangements by mounting a segment of the array in place of the experimental cryosurface. The source of incident gas could be either (1) the large nozzle, (2) a small high pressure jet for large expansions, or (3) a high temperature jet, depending upon the application intended for the cryoarray. The canister system for determining the fraction captured could be used as in the present tests. This procedure would permit evaluation of a pumping system within a limited time and cost. The lack of pitot tube viscous correction data at low Reynolds number is an impediment to the accurate calibration of low density supersonic nozzles.

The lower temperatures (5 to 16°K) obtainable with liquid helium were not useful in improving the cryopumping effectiveness for the test gases used in this program. Since evaporation of the frosts was negligible at temperatures less than 30°K, the gaseous helium refrigerator provided a superior coolant to liquid helium.

The shock wave ahead of a blunt body will disappear when the condensation fraction is greater than 90 percent by some undetermined amount.

REFERENCES

1. Collins, J. A., Anderson, D. E., and Clement, W. D. "Modification of Supersonic Flow Fields under Near Space Conditions." AEDC-TDR-64-66 (AD601089), June 1964.

2. Collins, J. A. "Capture Coefficients and Shock Structure for a LHe and LNe Cooled Cryoplate in a Mach 3 Low Density Air Stream." AEDC-TDR-64-124 (AD601376), June 1964.

3. Collins, J. A. and Anderson, D. E. "Cryopumping of a High Velocity Gas at Knudsen No. Near 0.1." American Institute of Aeronautics and Astronautics Annual Meeting, Los Angeles, June 1964.

4. Collins, J. A. and Triplett, M. J. "Condensation of a Rarefied Supersonic Flow on a Cold Surface." Fourth International Symposium on Rarefied Gas Dynamics, Toronto, July 1964.

5. Schlichting, H. Boundary Layer Theory. McGraw-Hill, New York, 1955.

6. Private Communication with Hill, D. and Pinion, E. "Investigation of the Internal Flow Characteristics of Two Types of ALARR High Altitude Air Sampling Probes in Supersonic Low Density Airstreams."

7. Data Book. Thermophysical Properties Research Center, Purdue Research Foundation, Layfayette, Ind.

8. Dushman, S. and Lafferty, J. Scientific Foundations of Vacuum Technique. John Wiley and Sons, New York, 1962.

9. Loeb, L. The Kinetic Theory of Gases. Dover Publications, New York, 1961.

10. Handbook of Chemistry and Physics. Chemical Rubber Publishing Co., Cleveland, Thirty-Seventh Edition, 1957-58.

11. Flynn, T. M., Draper, J. W., and Roos, J. J. "The Nucleate and Film Boiling Curve of Liquid Nitrogen at One Atmosphere." Advances in Cryogenic Engineering, Plenum Press, New York, 1961 Edition, pp. 539-545.

12. Cassanova, R. A. and Stephenson, W. B. "Expansion of a Jet into Near Vacuum." AEDC-TR-65-151 (AD469041), August 1965.

13. Boison, J. C. and Curtiss, H. A. "An Experimental Investigation of Blunt Body Stagnation Point Velocity Gradient." American Rocket Society Journal. Volume 29, No. 1, January 1959, p. 130.

APPENDIXES

I. ILLUSTRATIONS

II. CORRELATION OF SHOCK DETACHMENT DISTANCE WITH CONDENSATION FRACTION

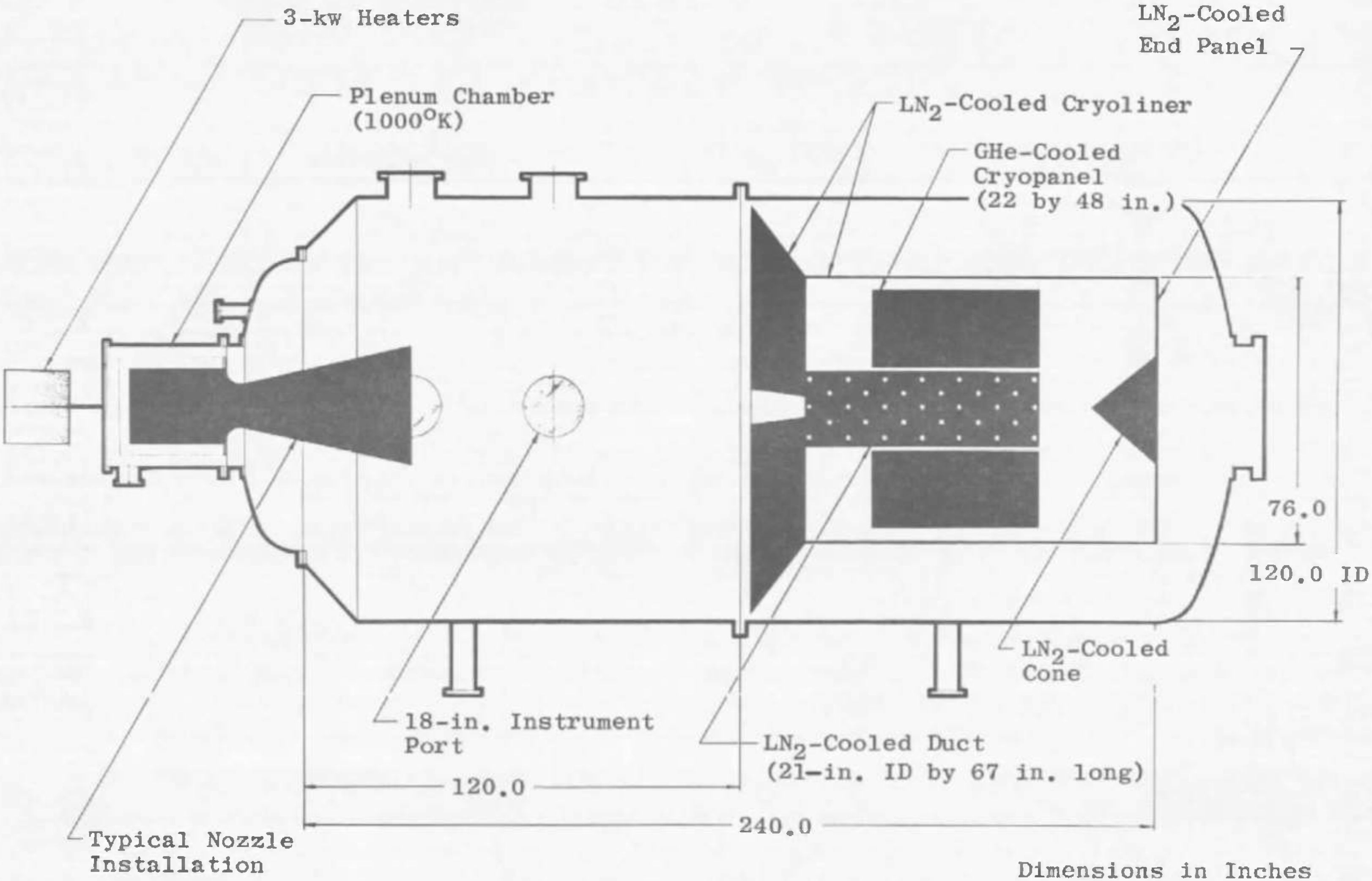

Fig. 1 Modified ARC 8V Chamber

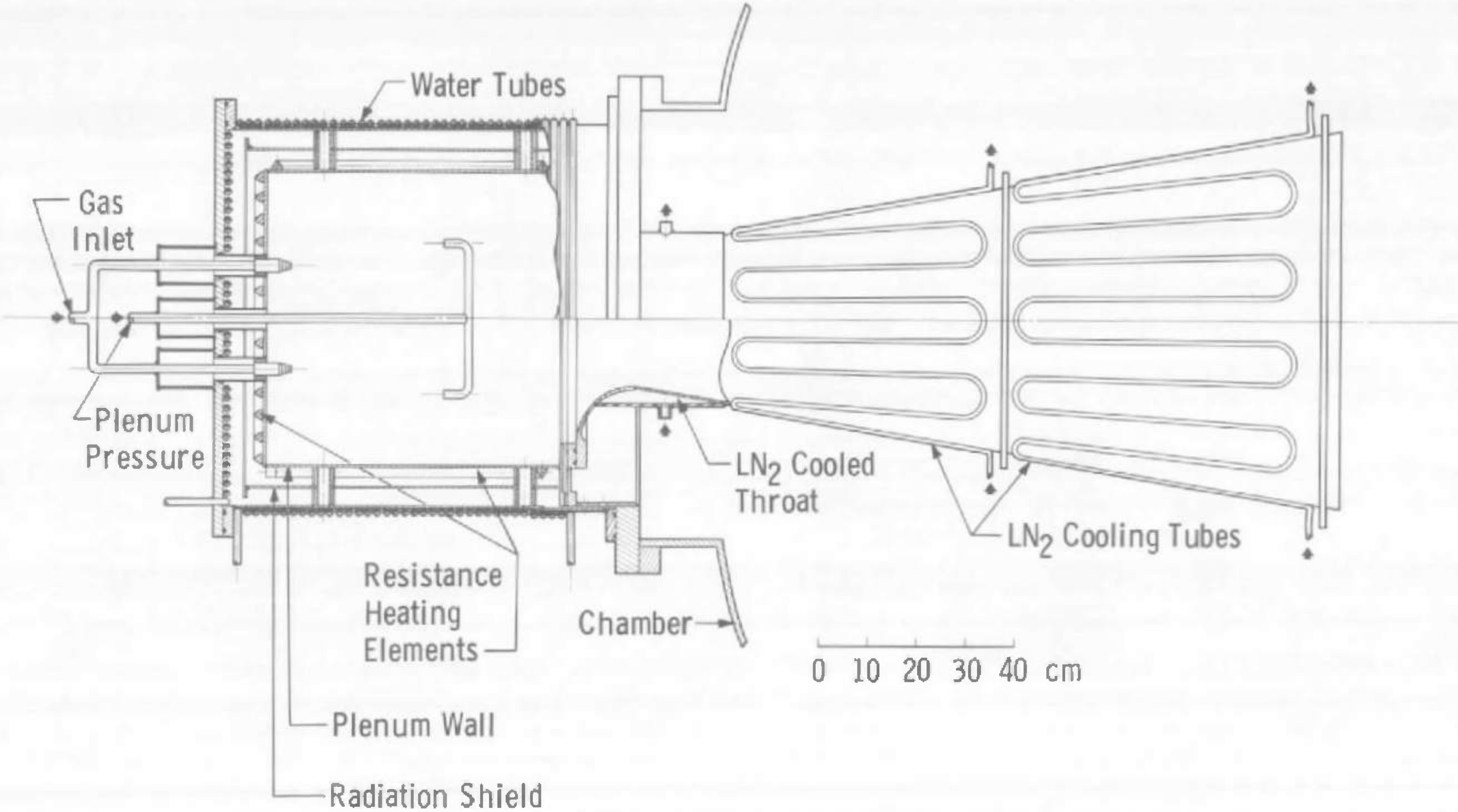

Fig. 2 M = 3 Low Density Nozzle

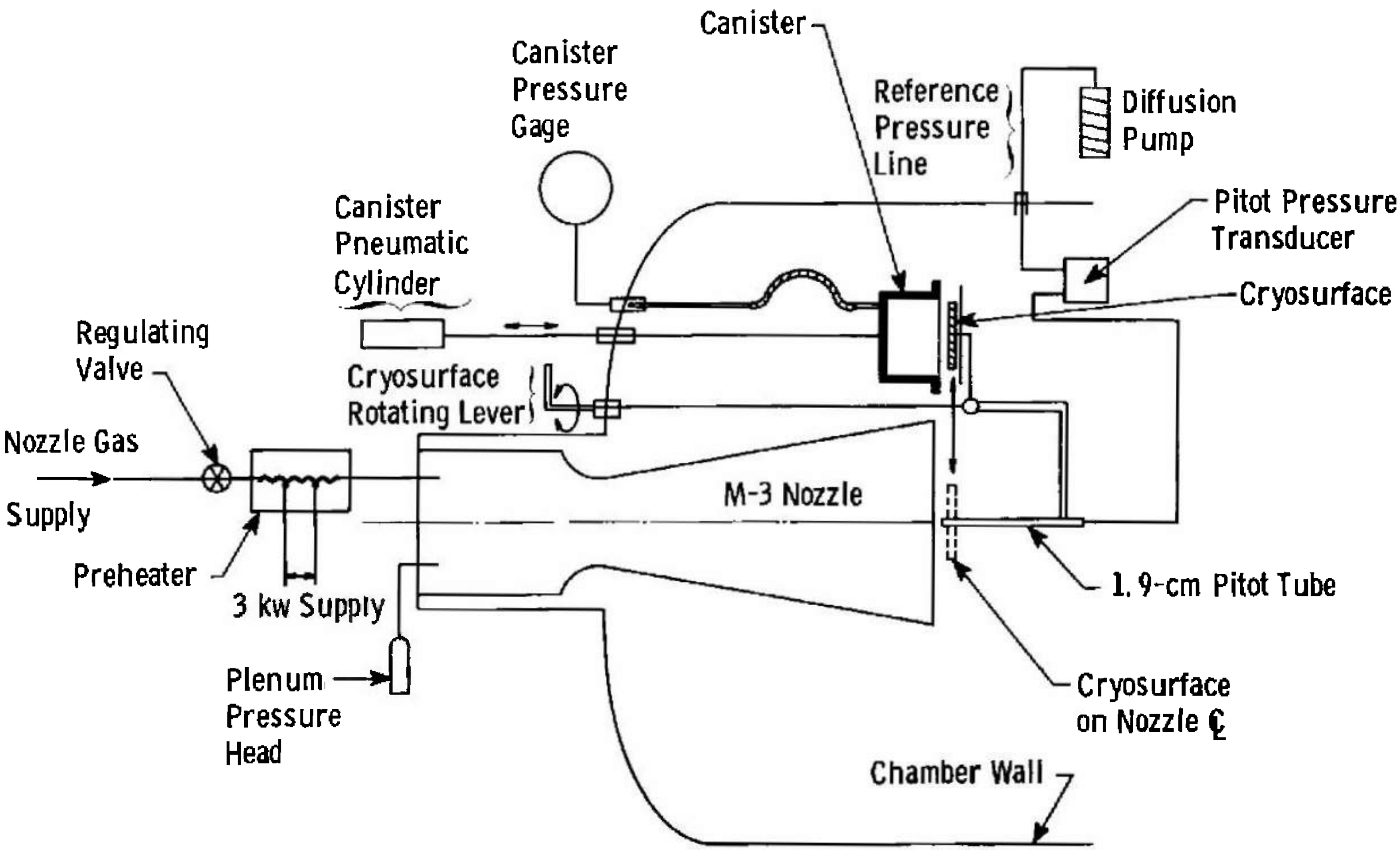

Fig. 3 Schematic of Test Installation

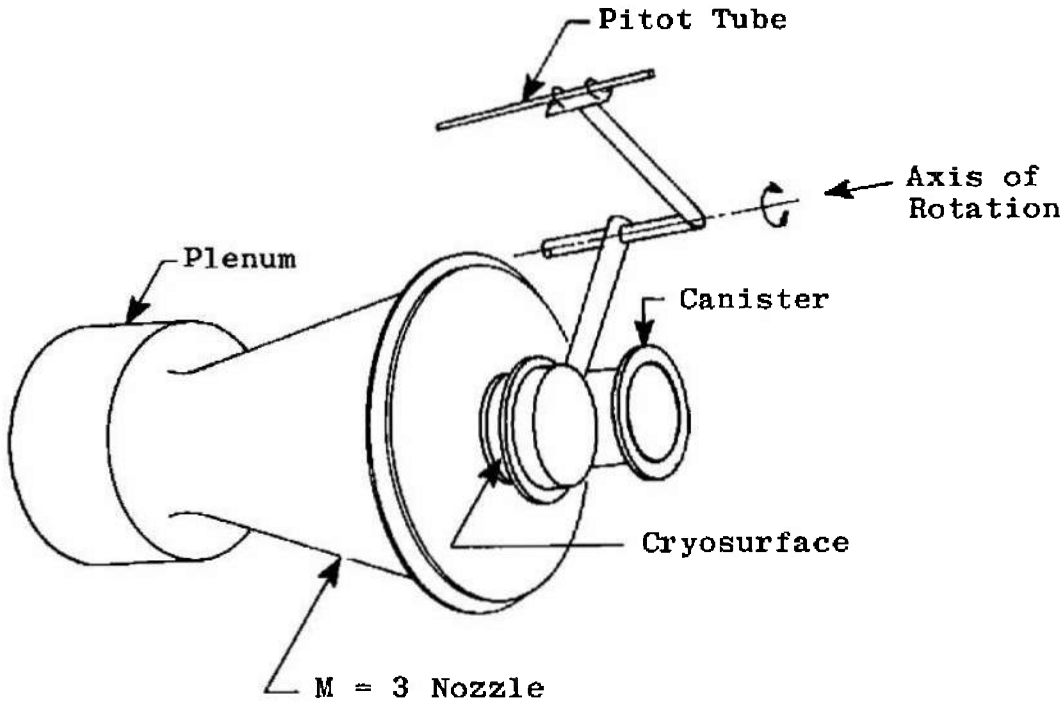

Fig. 4 Cryosurface, Pitot Tube, and Canister

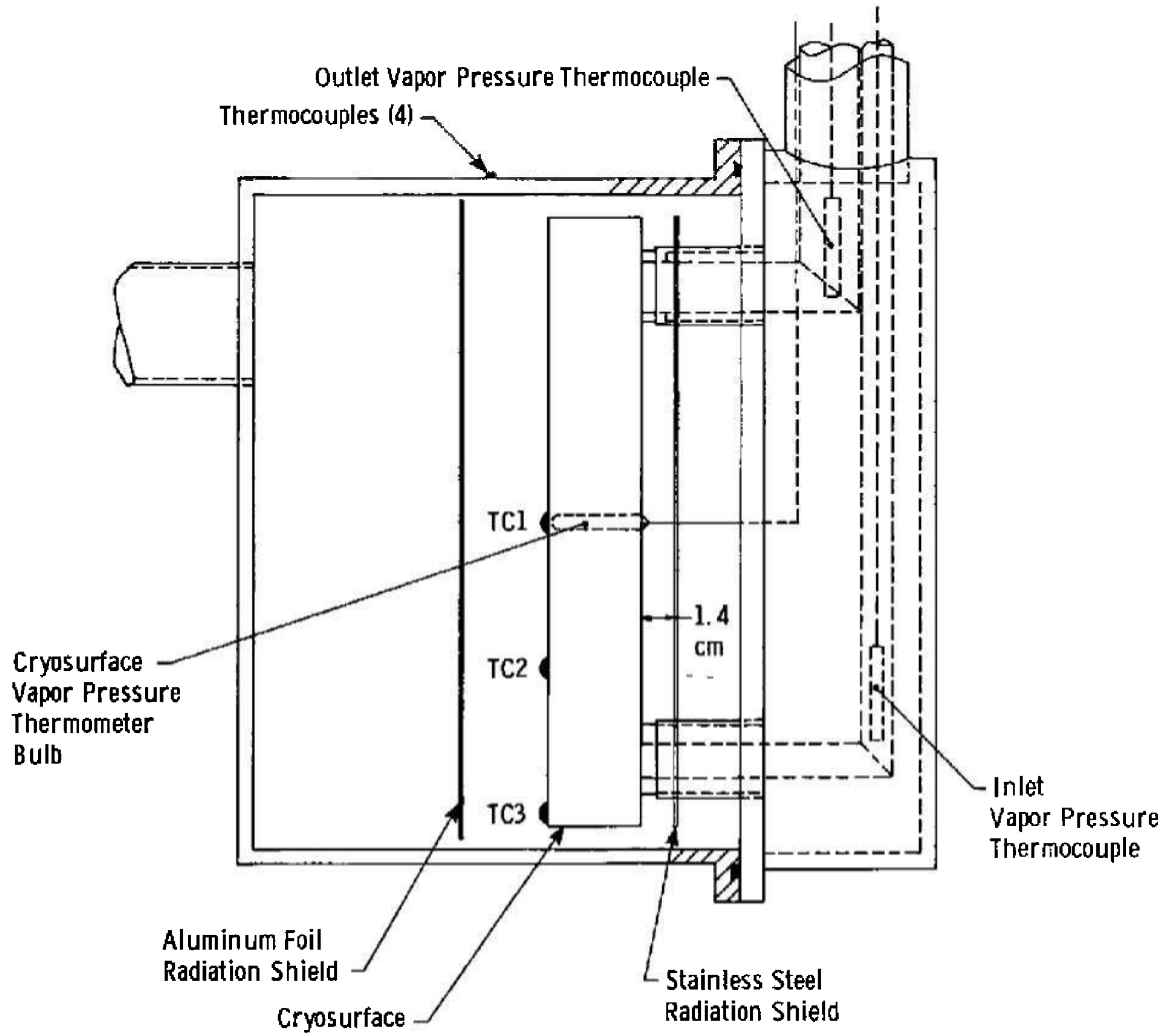

Fig. 5 Cryosurface in Canister

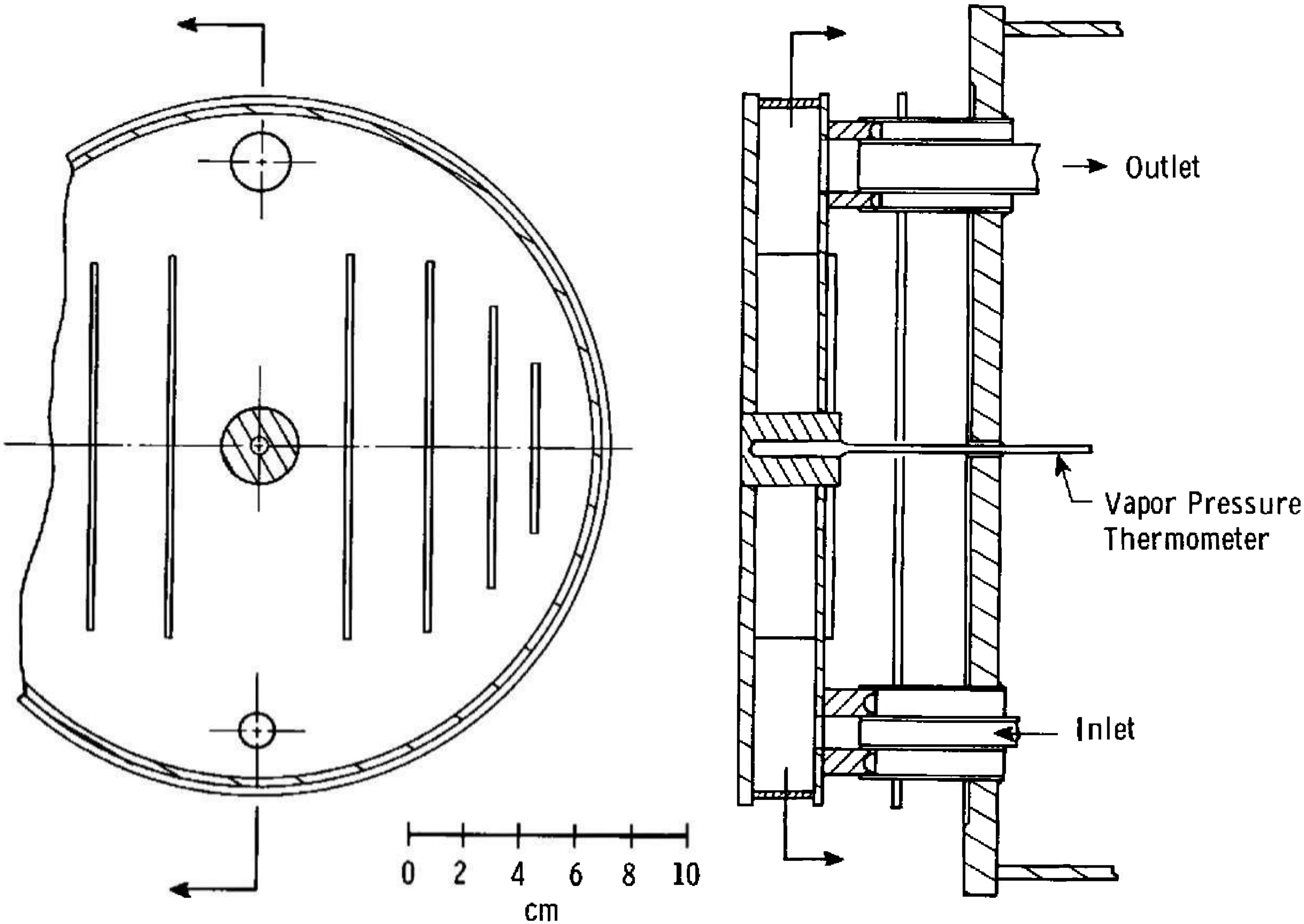

Fig. 6 Cryosurface Construction

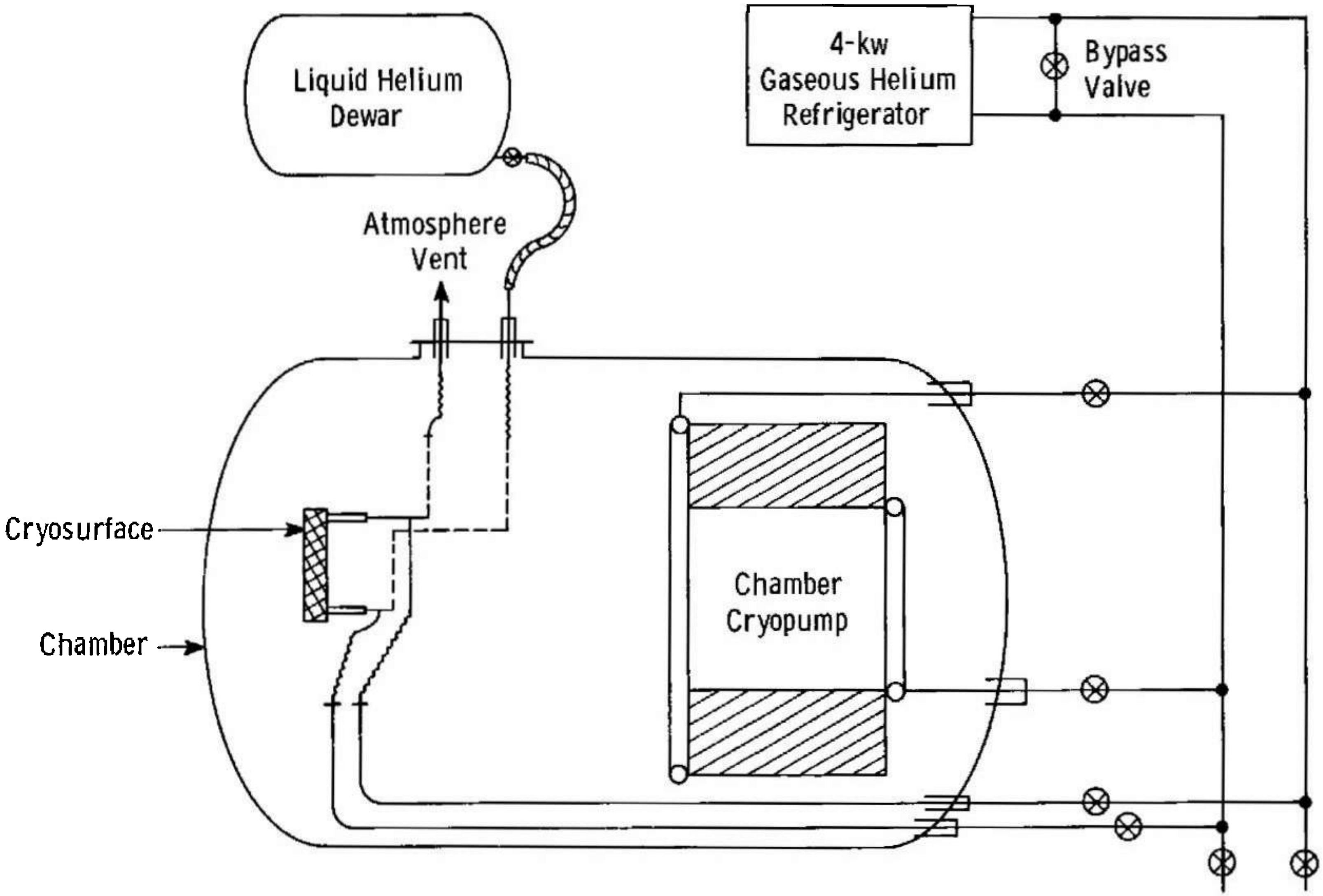

Fig. 7 Schematic of Cryogenic System

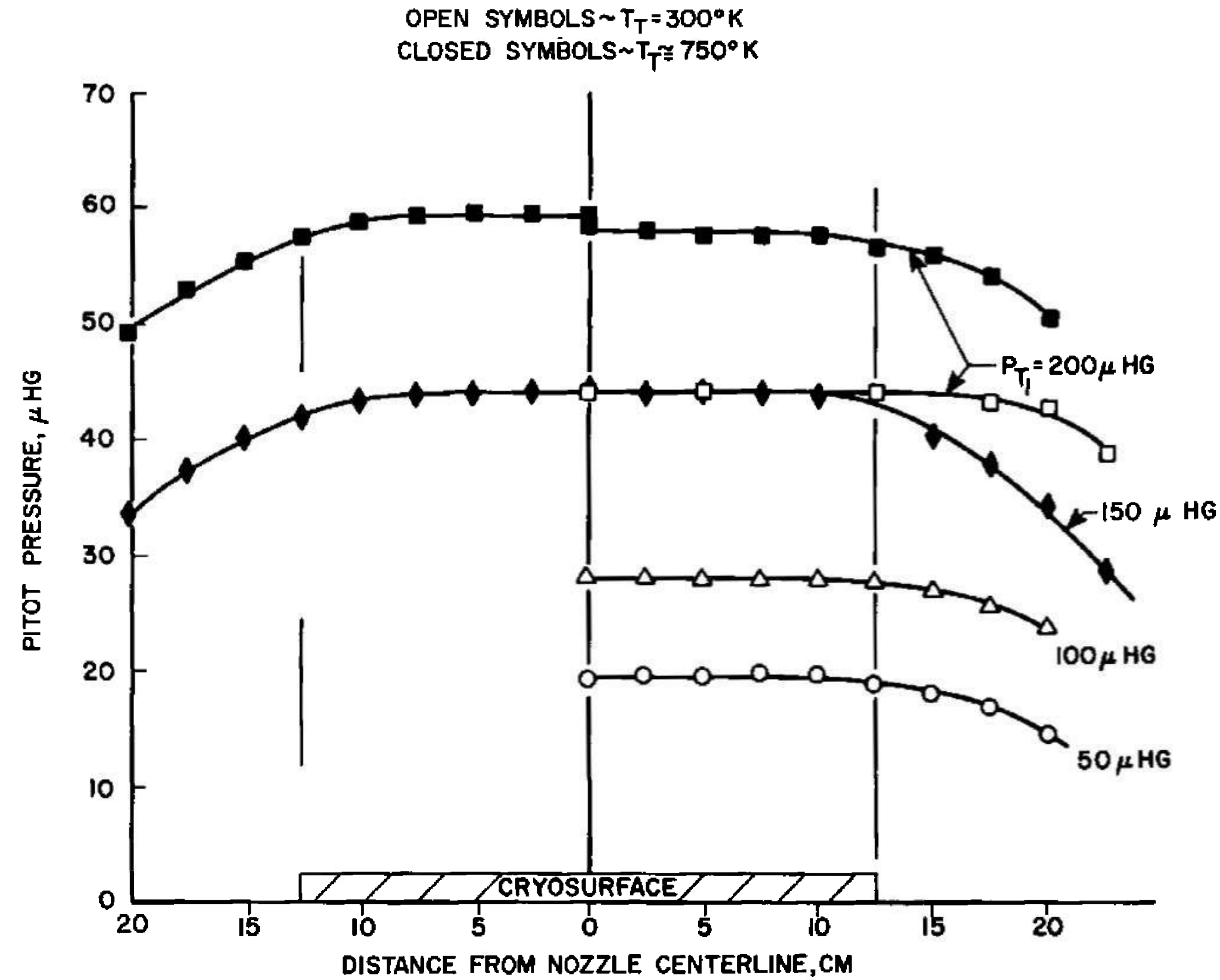

Fig. 8 Nitrogen Flow Pitot Profiles

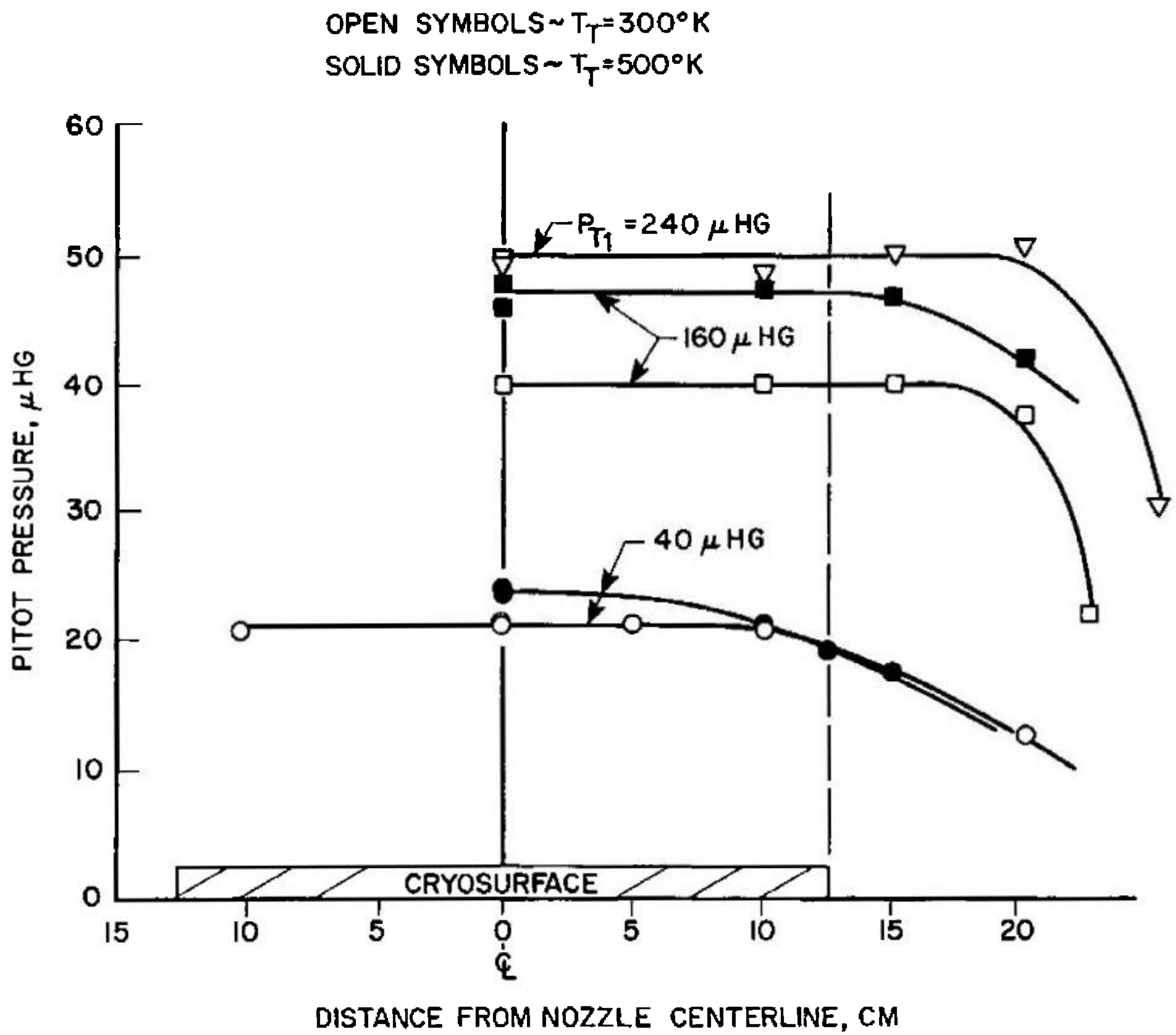

Fig. 9 Argon Flow Pitot Profiles

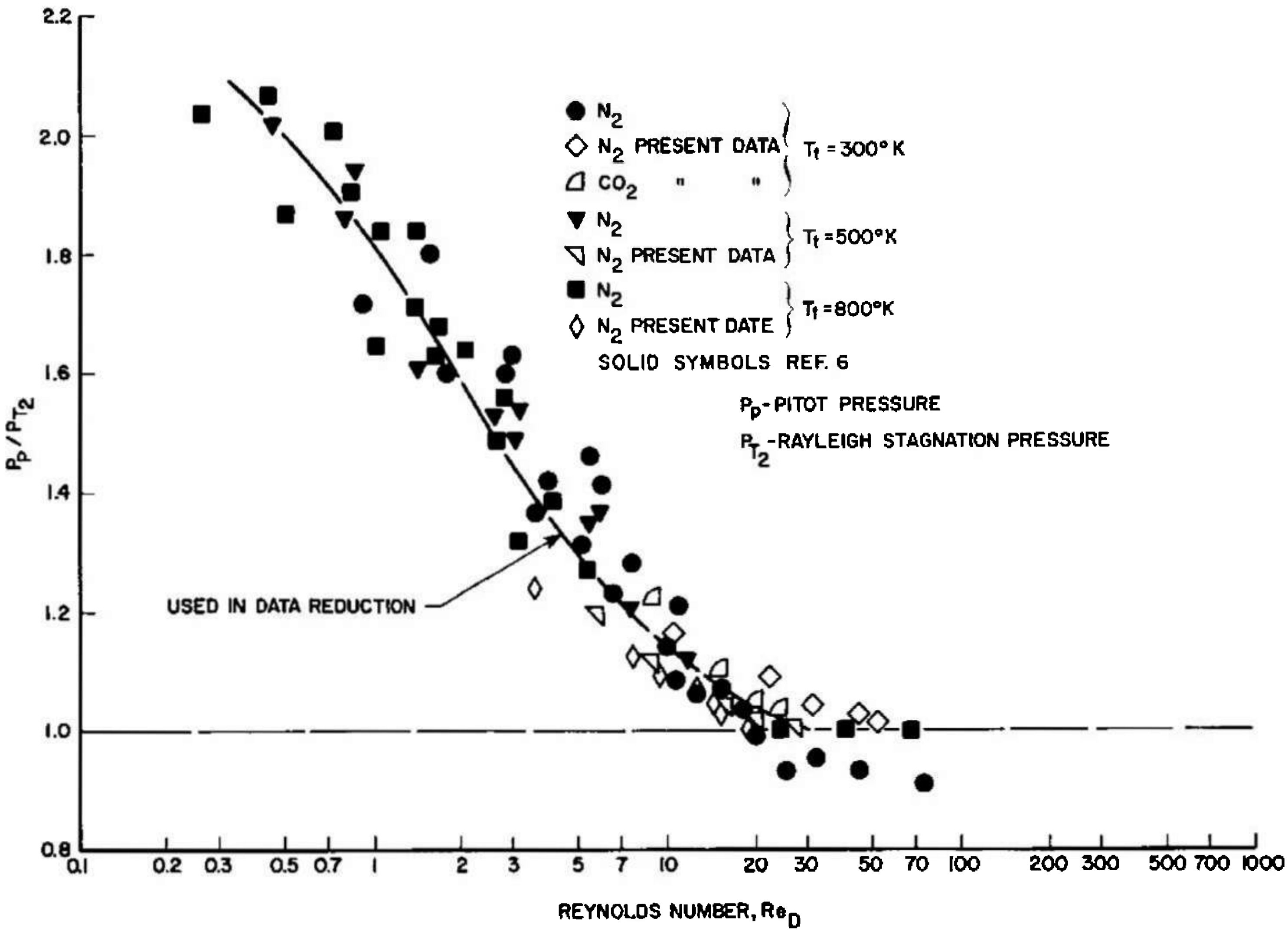

Fig. 10 Pitot Tube Viscous Effect

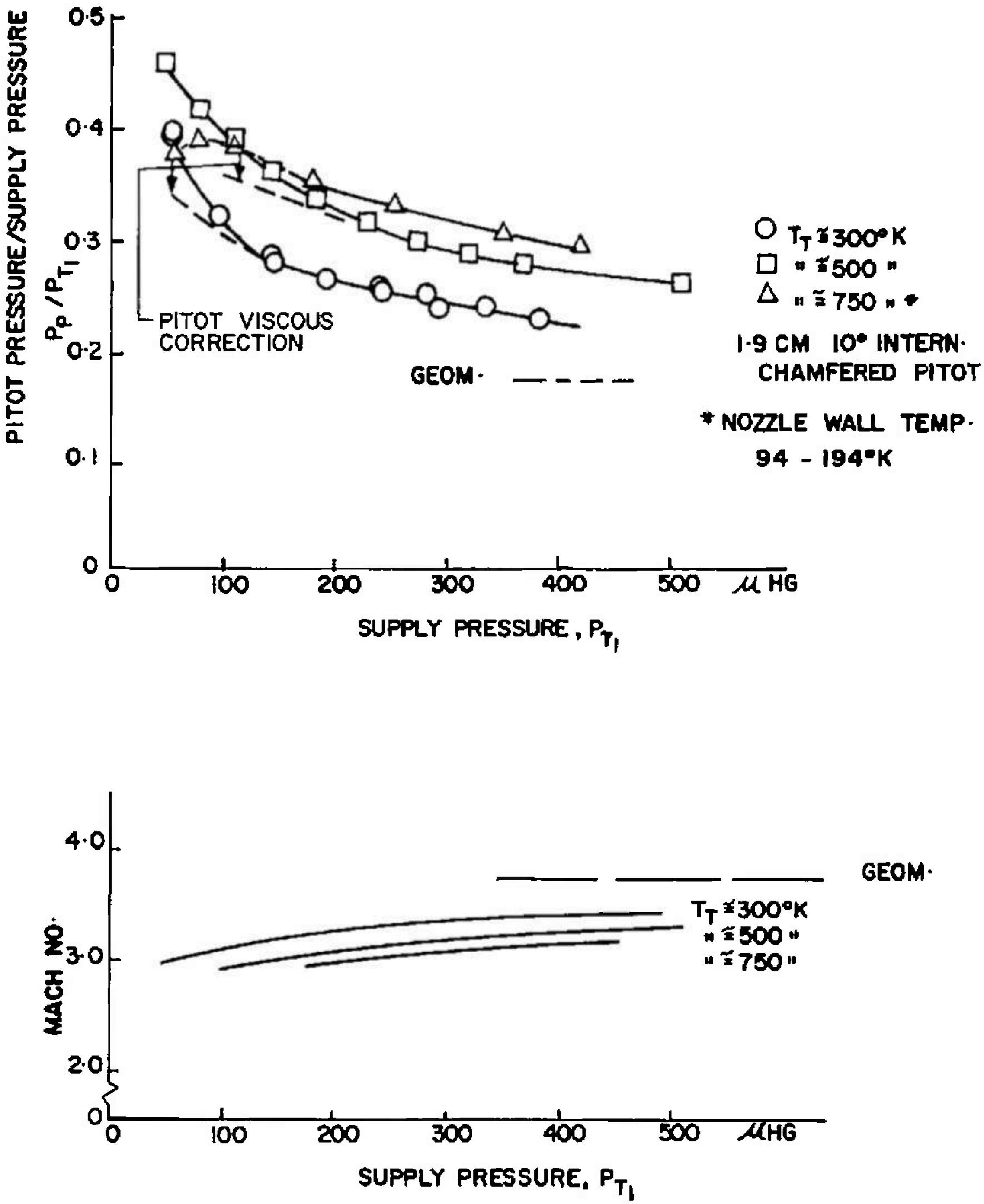

Fig. 11 M = 3 Nozzle Calibration with Nitrogen

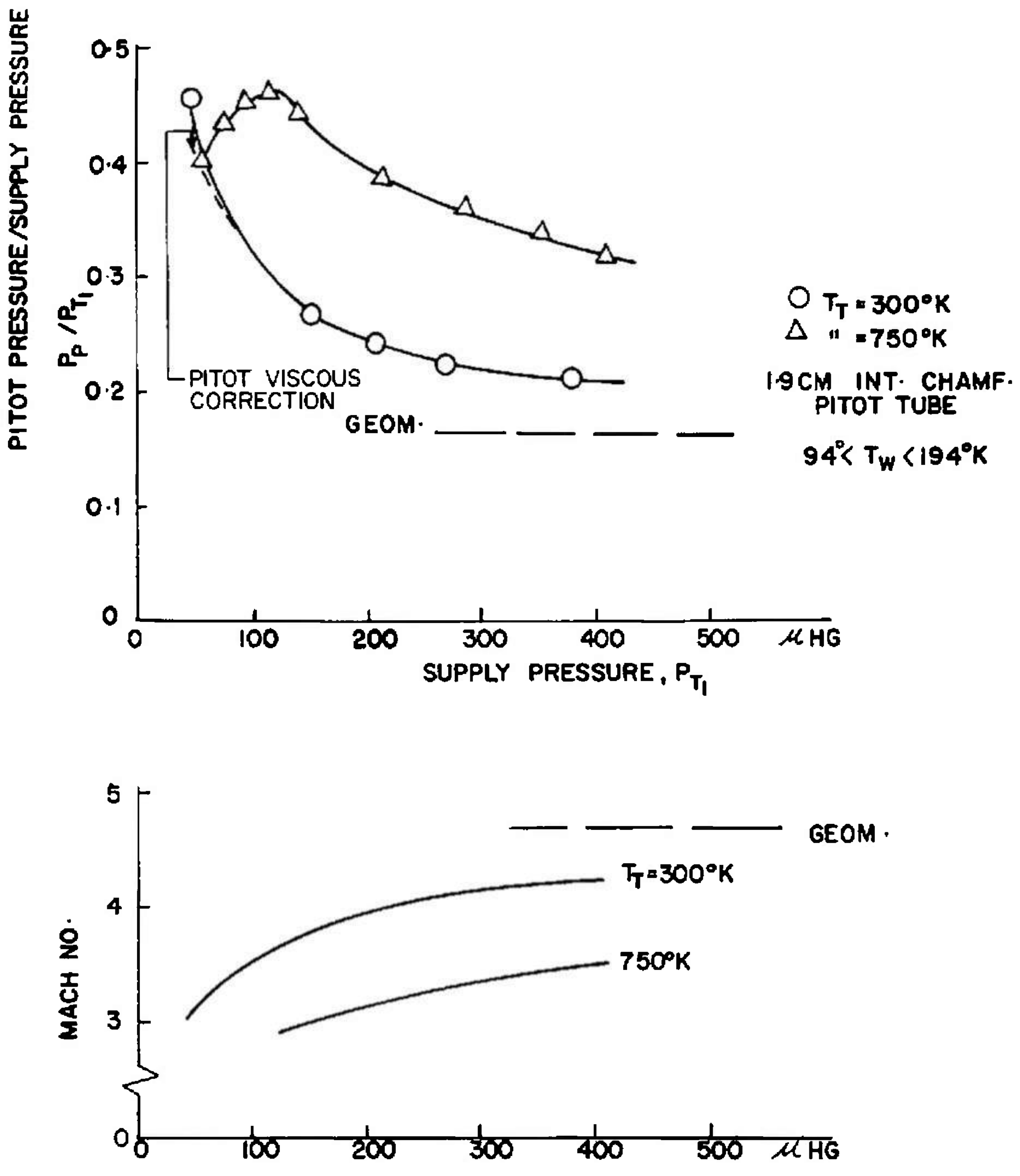

Fig. 12 M = 3 Nozzle Calibration with Argon

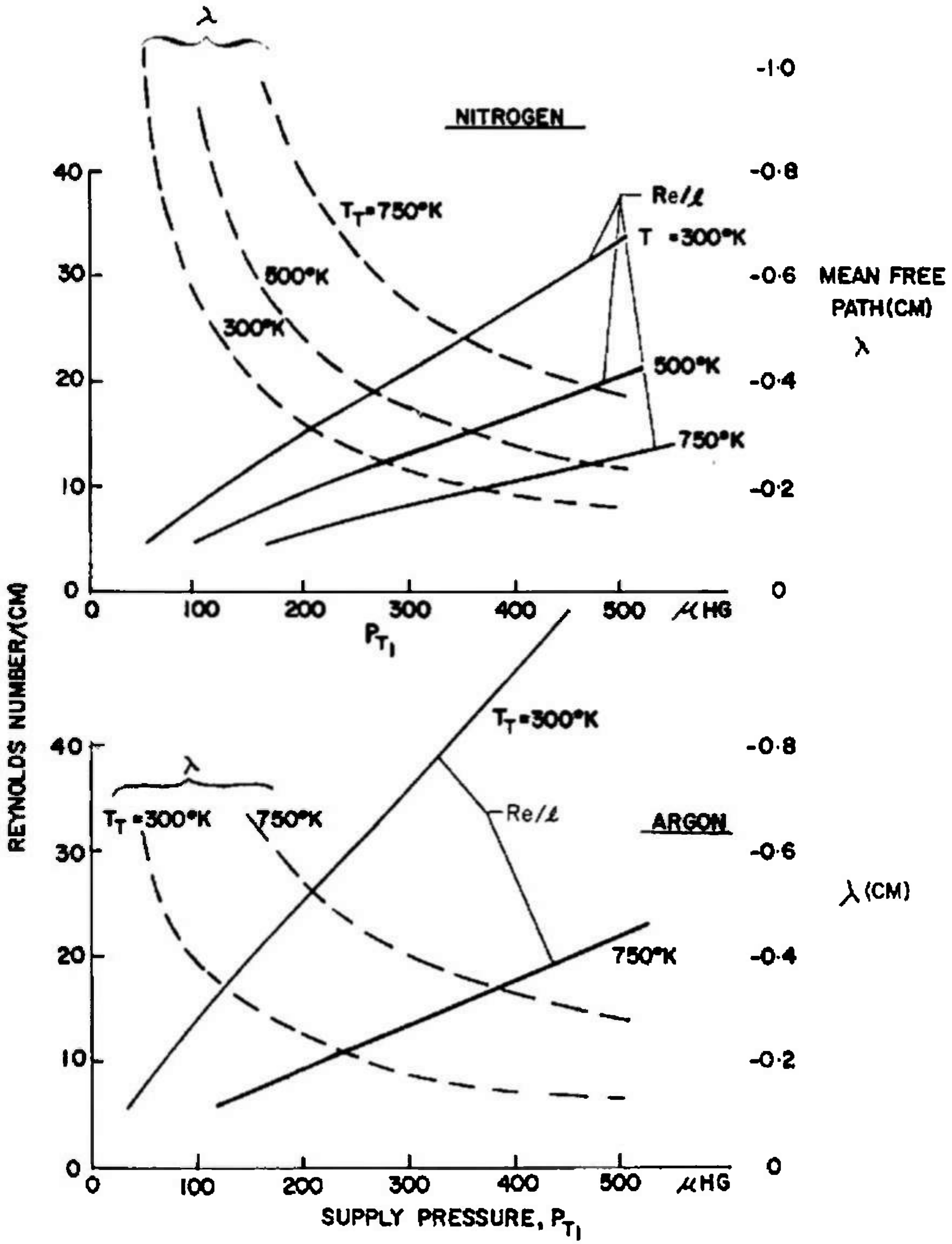

Fig. 13 Reynolds Number and Mean Free Path for M = 3 Nozzle

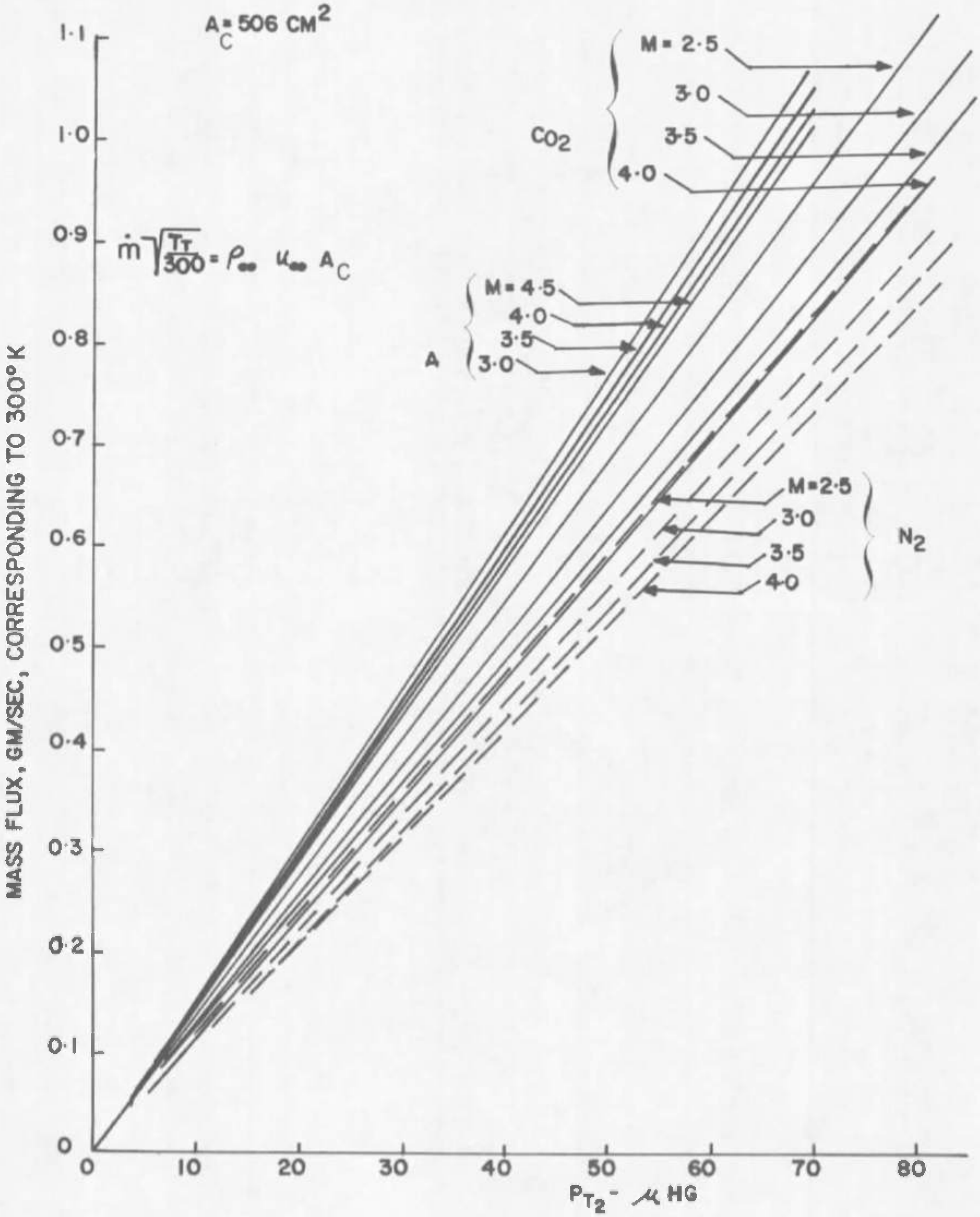

Fig. 14 Incident Flux versus Stagnation Pressure, P_{T_2}

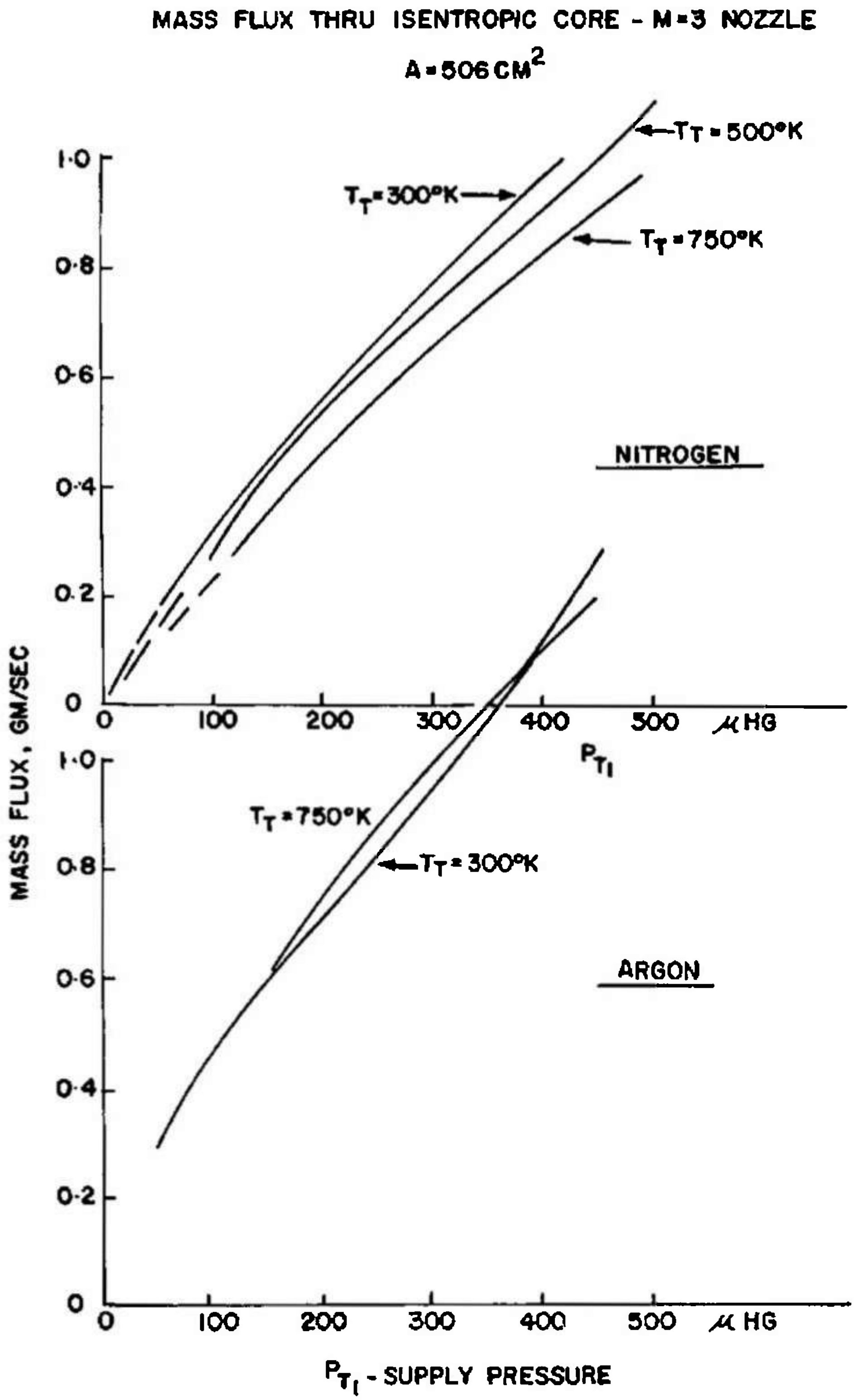

Fig. 15 Mass Flux through Isentropic Core with M = 3 Nozzle

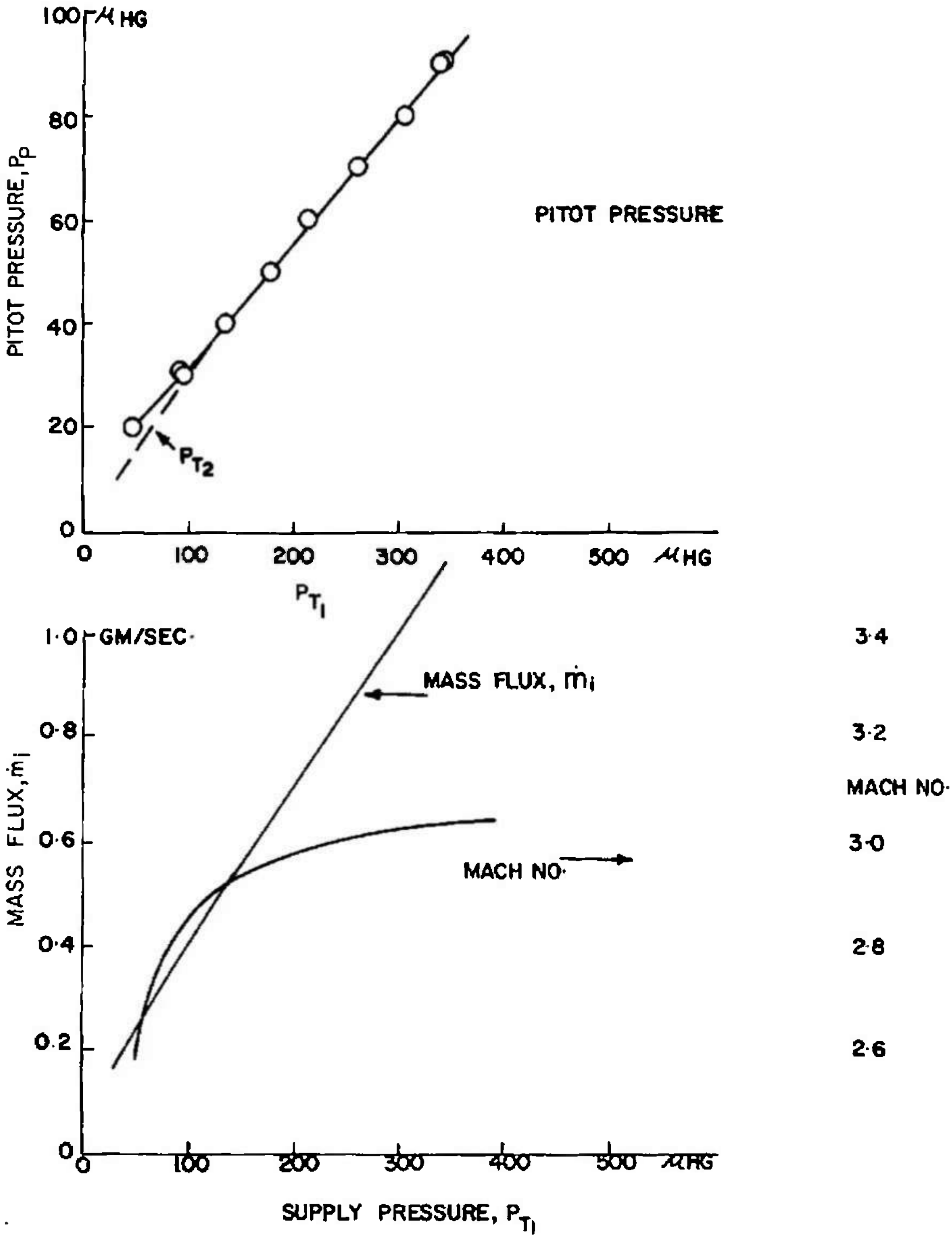

Fig. 16 M = 3 Nozzle Characteristics for CO_2 at 300°K

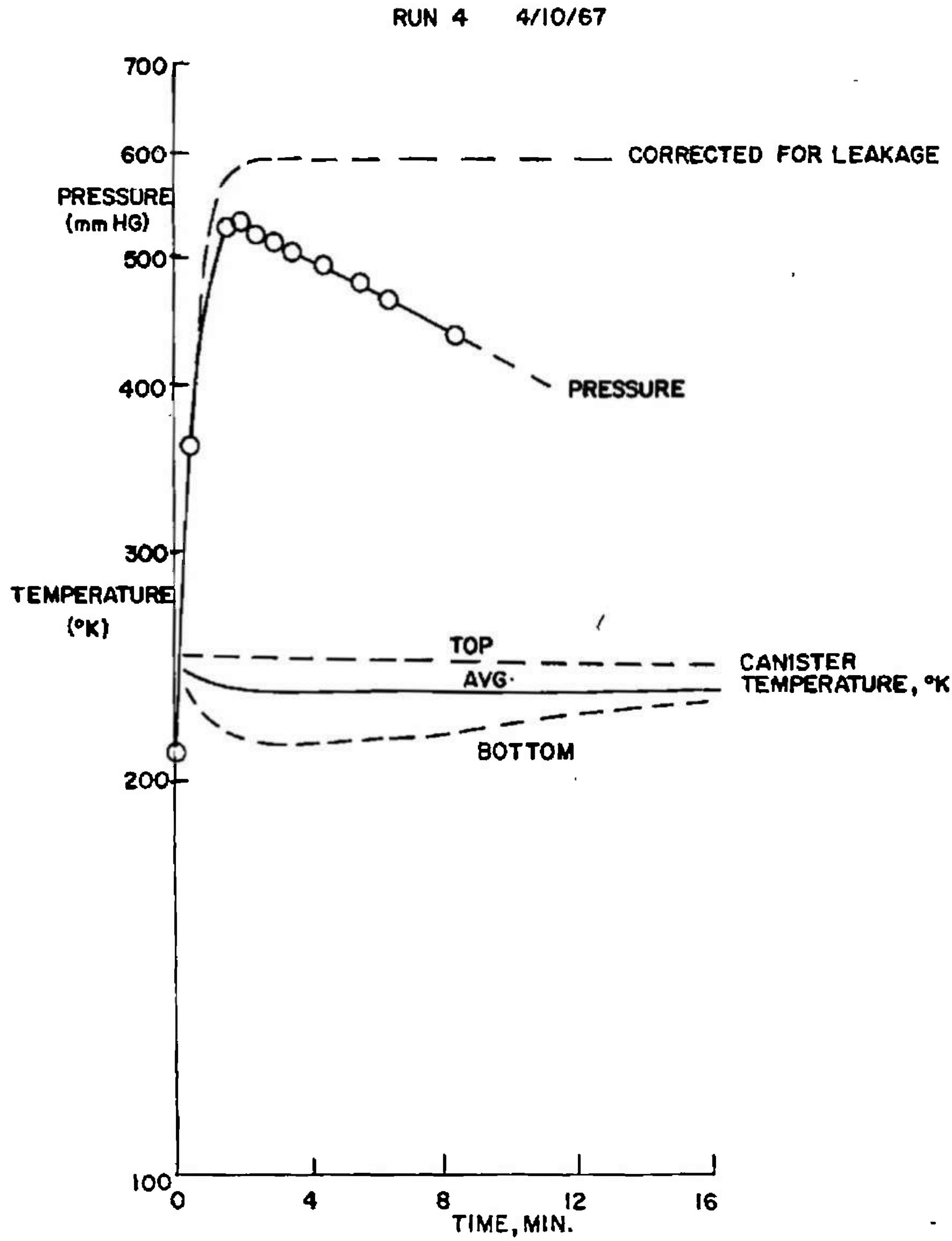

Fig. 17 Canister Pressure during Cryosurface Warmup (Leaking Seal)

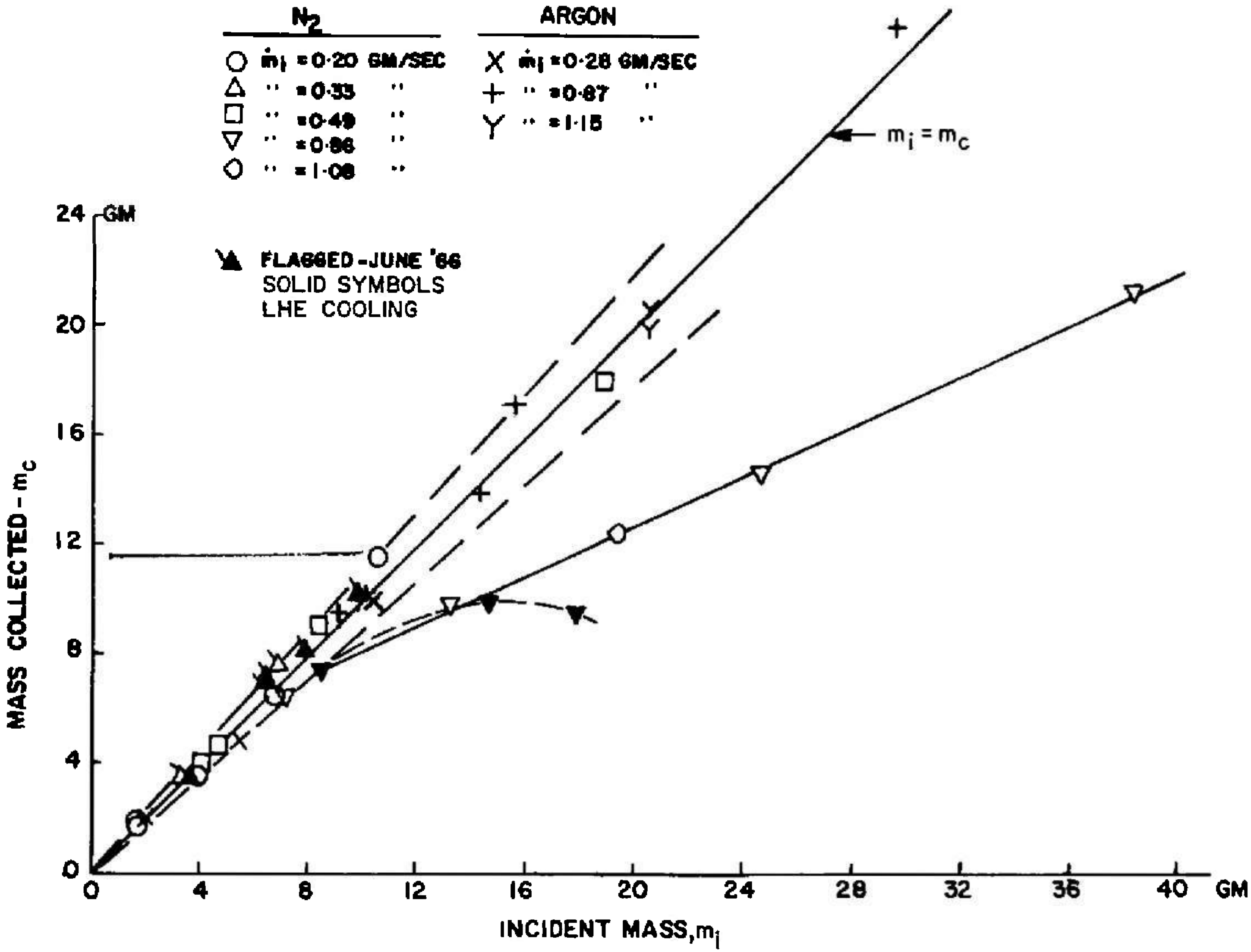

a. T_T = 300°K

Fig. 18 Cryosurface Gas Collection

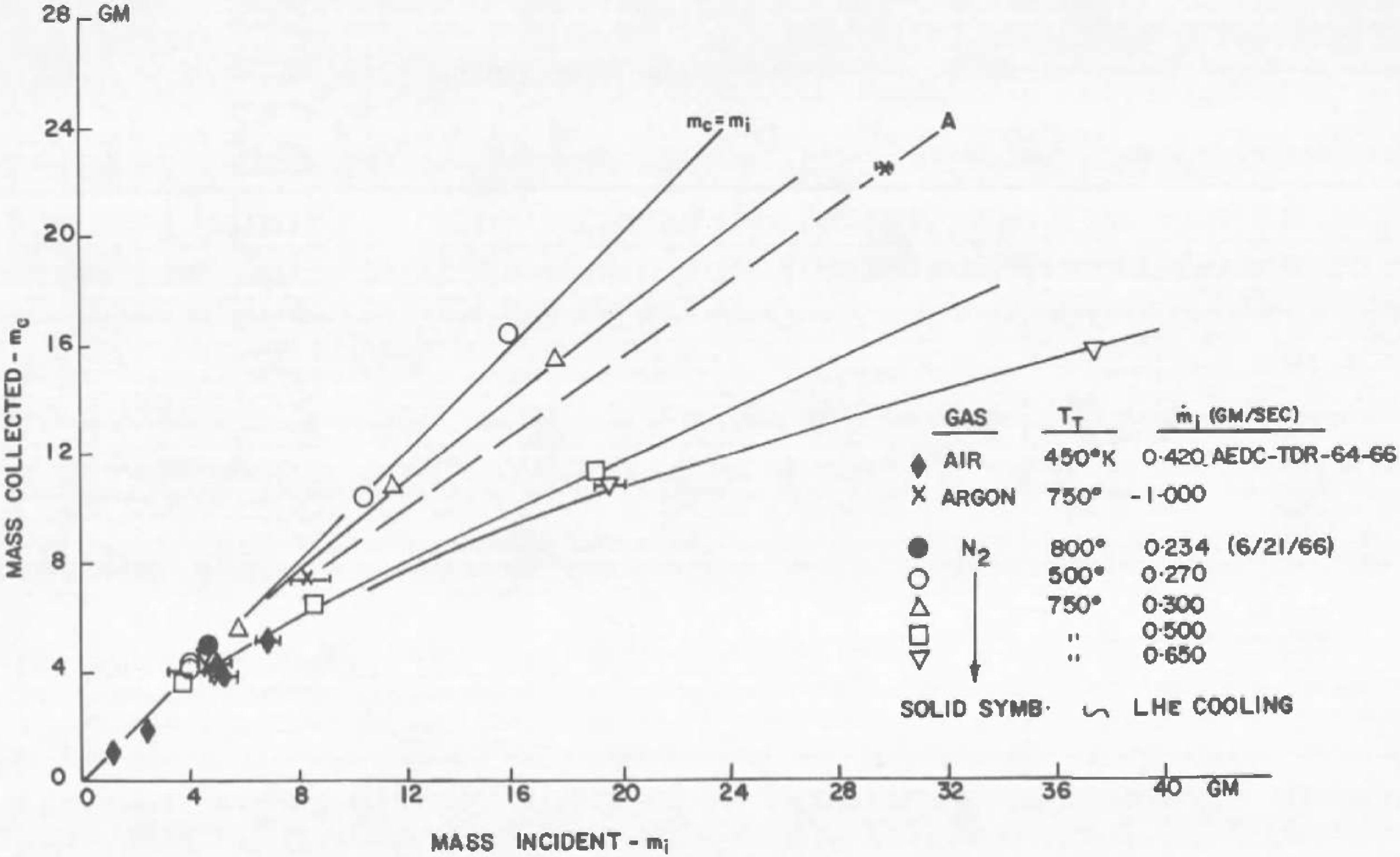

b. $500 < T_T < 750$ °K

Fig. 18 Concluded

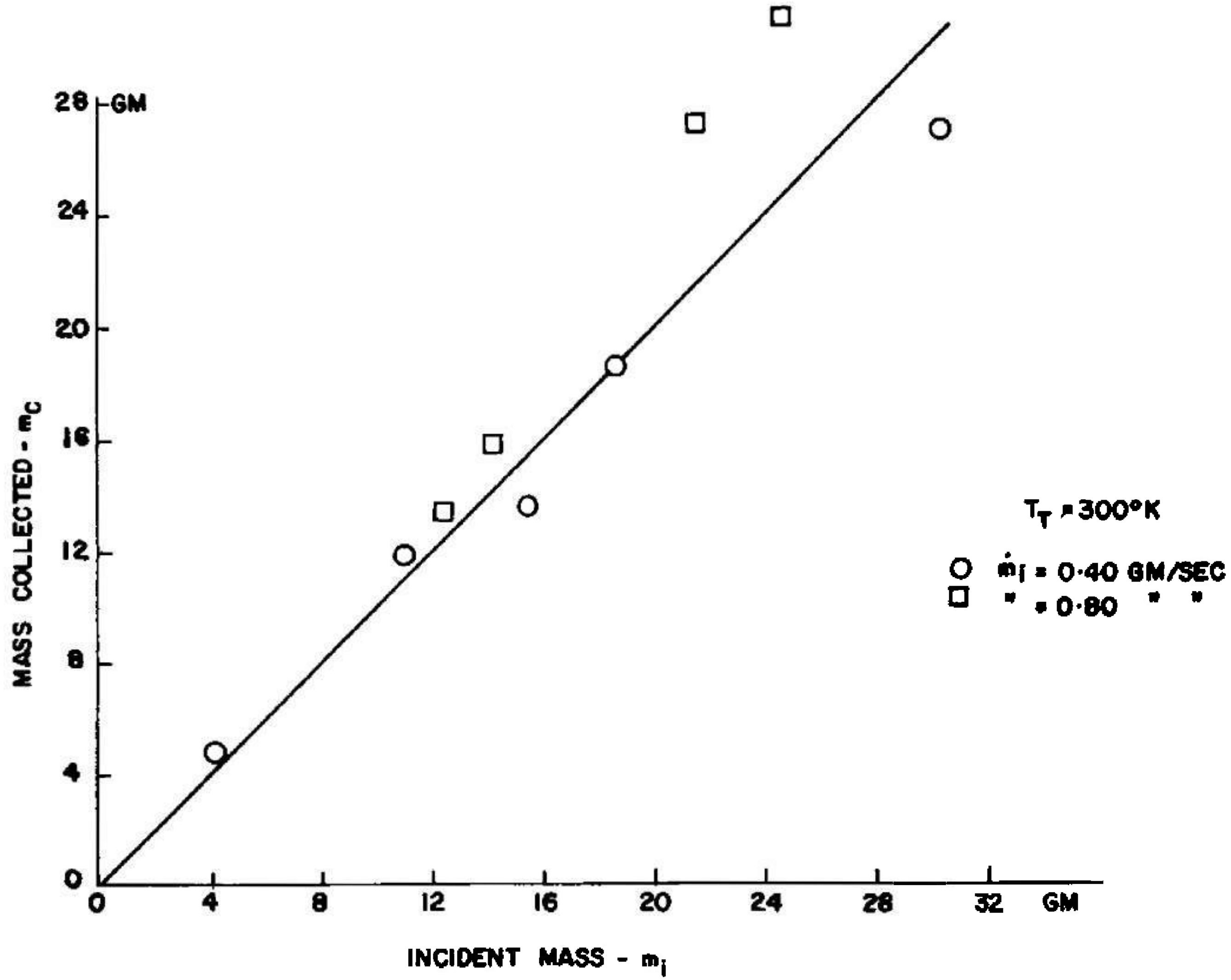

Fig. 19 Collection of CO_2 on LN_2-Cooled Cryosurface

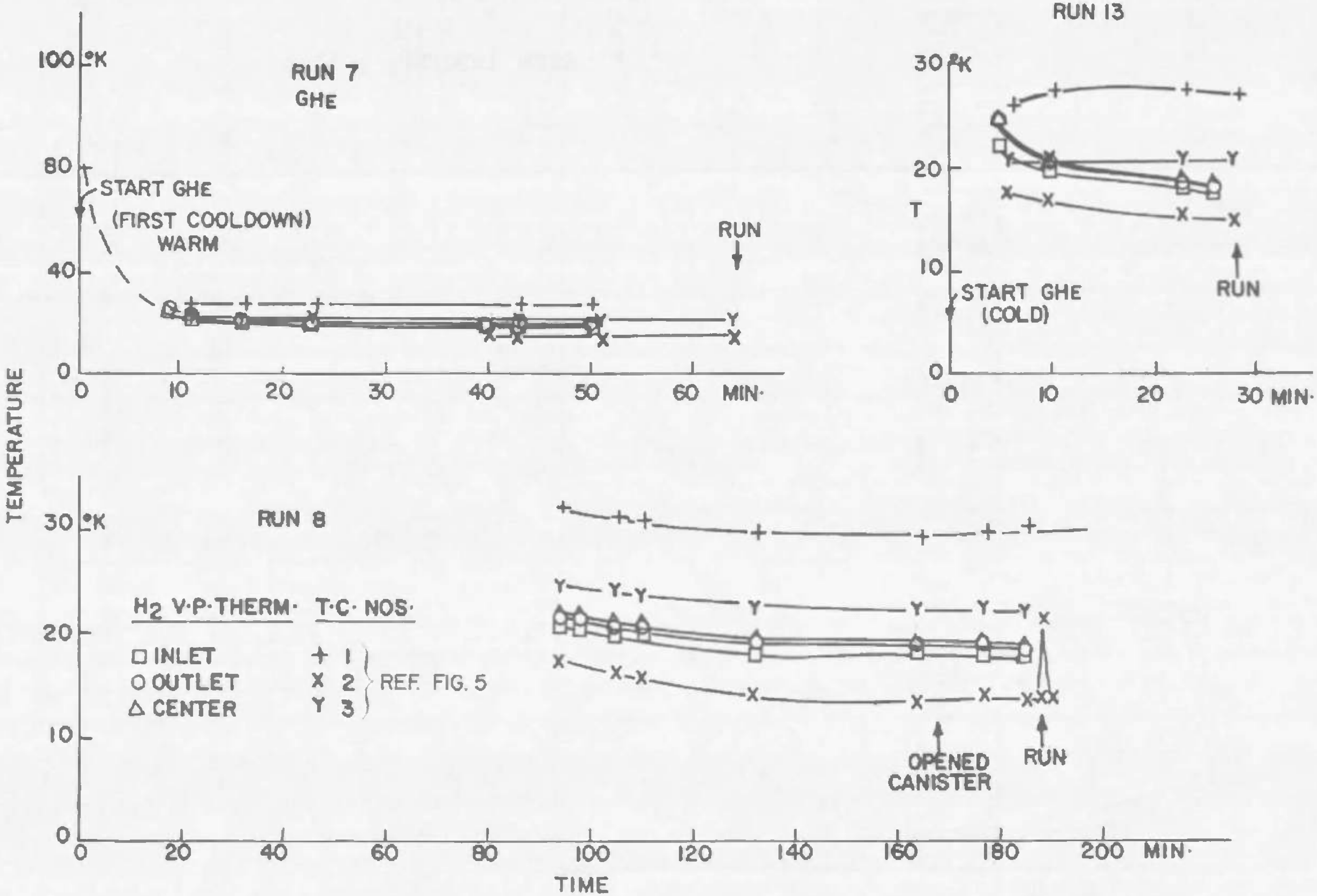

Fig. 20 Cryosurface Cooldown with Gaseous Helium

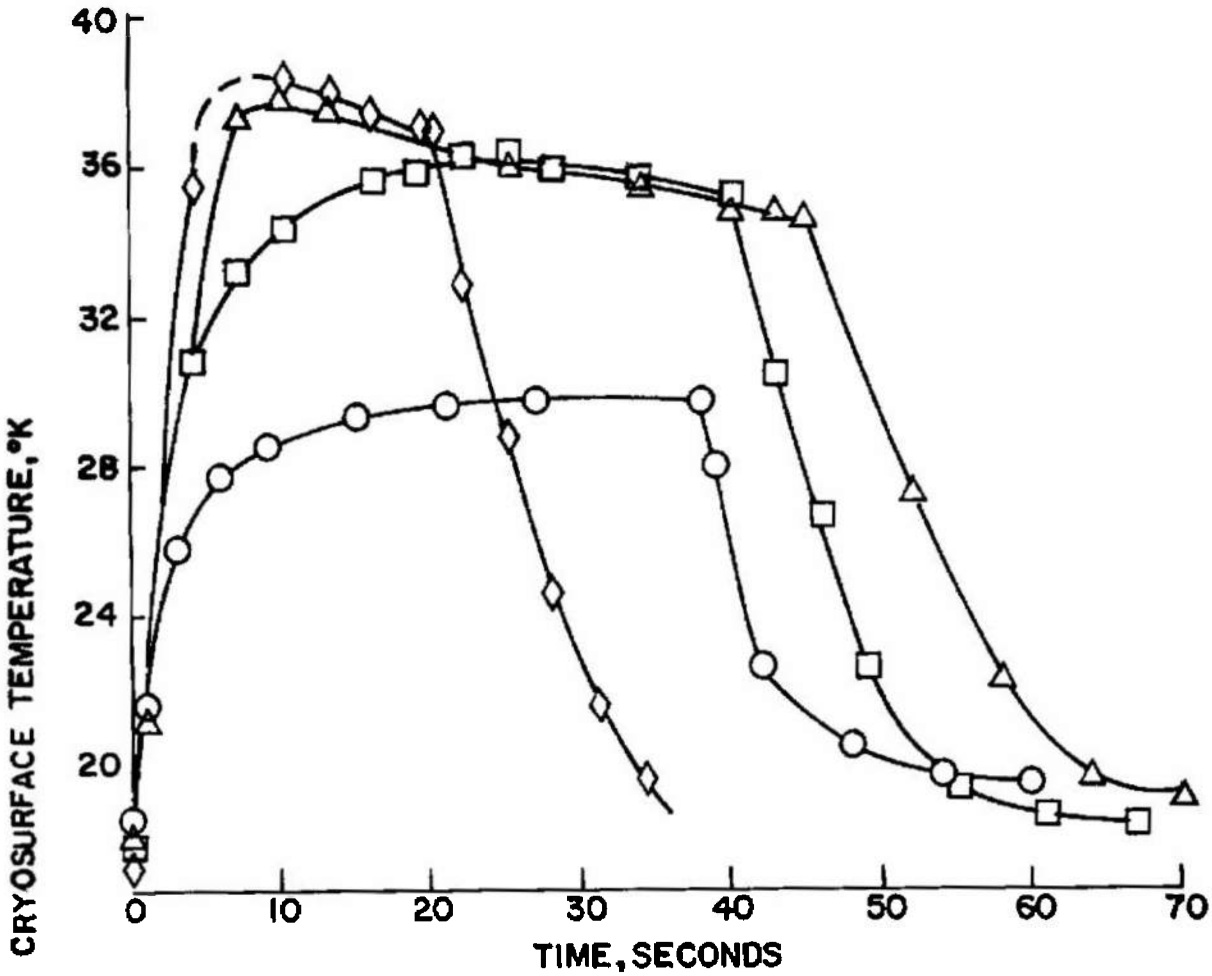

	RUN	T.C. NO.	CORR.*	$\dot{m}_i$	T_T
○	9	1	-10.0°K	0.185 GM/SEC	300°K
□	18	2	6.6 "	0.490 "	↓
△	13	2	-4.0 "	0.865 "	
◇	19	2	4.6 "	1.080 "	

* CORR. = T.C. - V.P. THERMOMETER AT START OF RUN

a. Runs 9, 13, 18, and 19 Surface Thermocouple Corrected by H_2 Vapor Pressure Thermometer

Fig. 21 Experimental Cryosurface Temperature - Time Variation

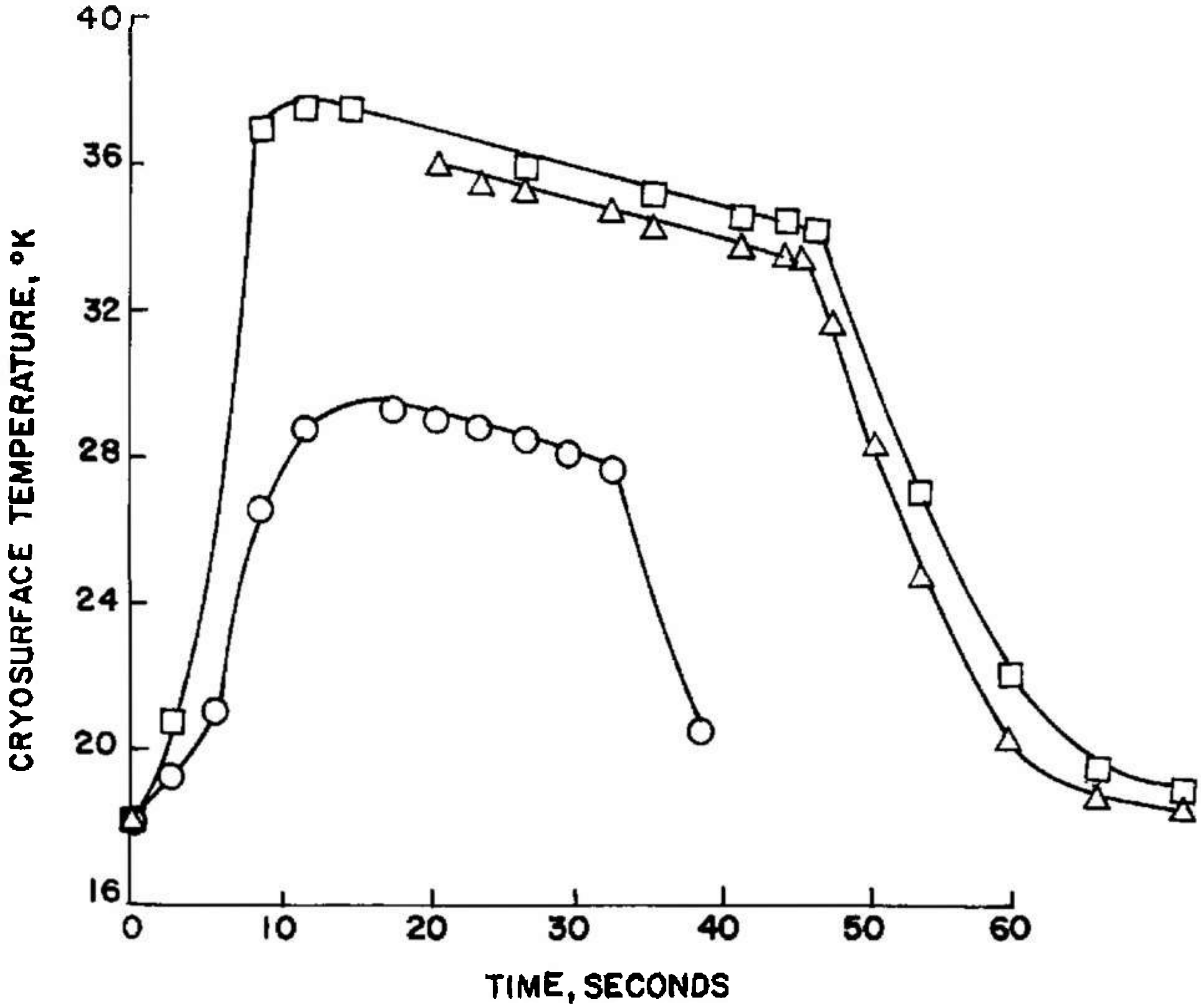

N_2, $\dot{m}_i = 0.865$ GM/SEC, $T_T = 300°K$

	RUN	T.C. NO.	CORR.
○	12	1	8.5°K
□	13	2	-4.0
△	14	2	-4.2

CORR. = $T_{TC} - T_{VP}$ AT 0 SEC.

b. Runs 12, 13, and 14

Fig. 21 Concluded

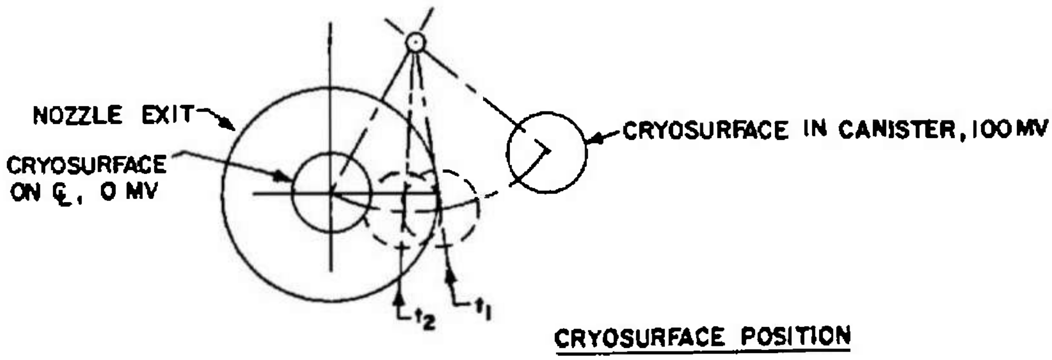

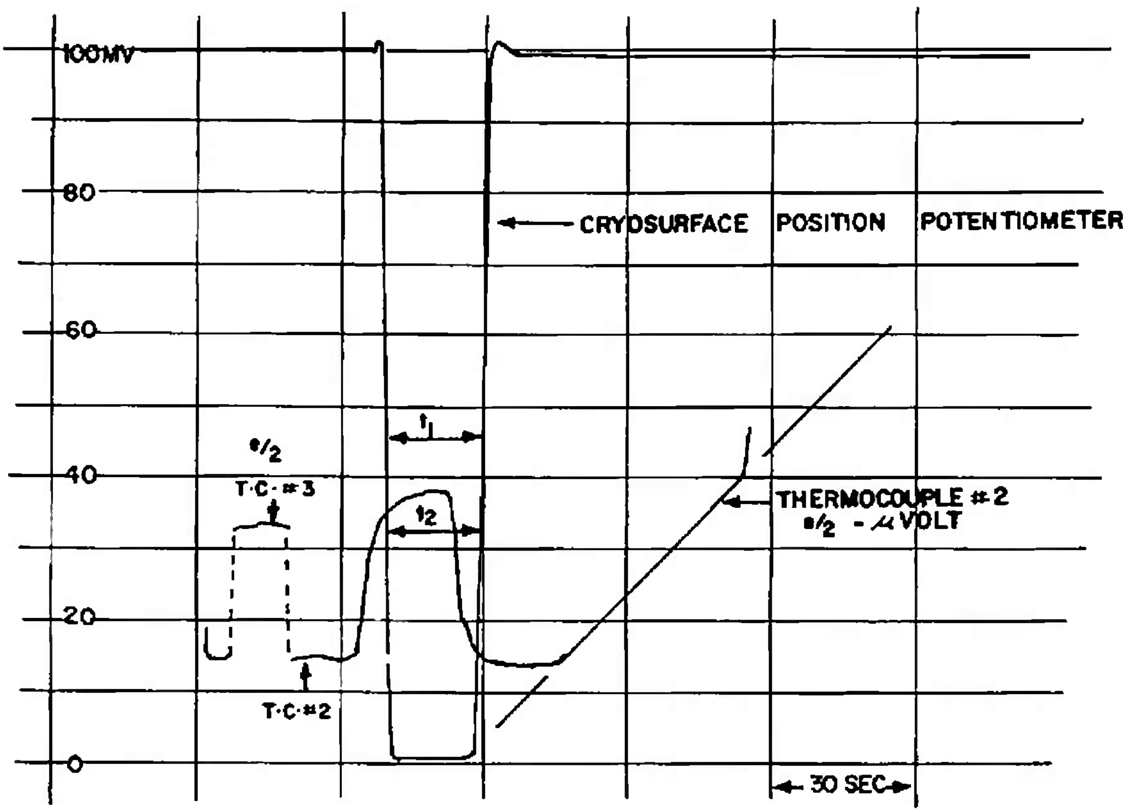

Fig. 22 Strip Recorder Trace of Data Record

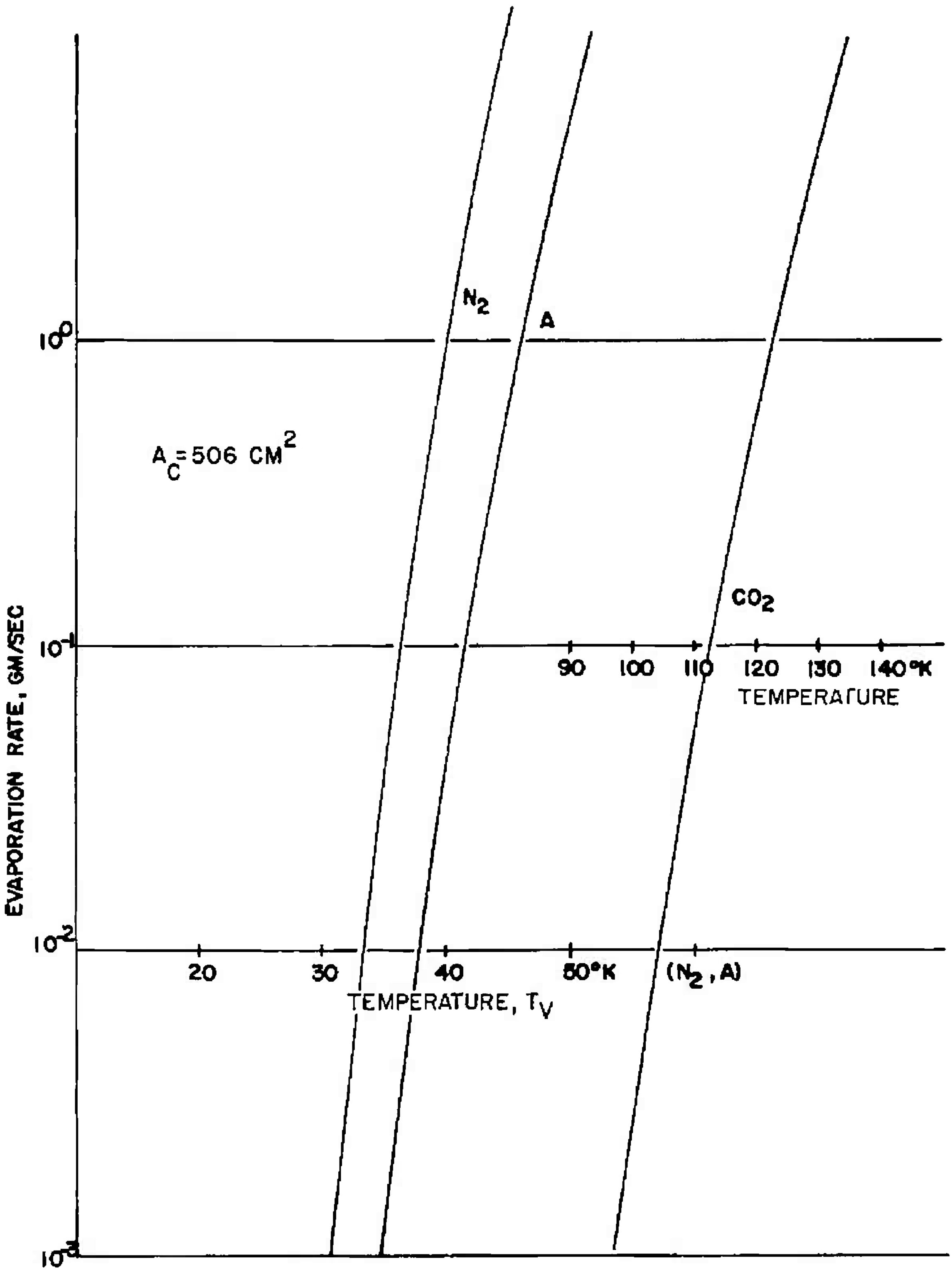

Fig. 23 Evaporation Rate of Frosts

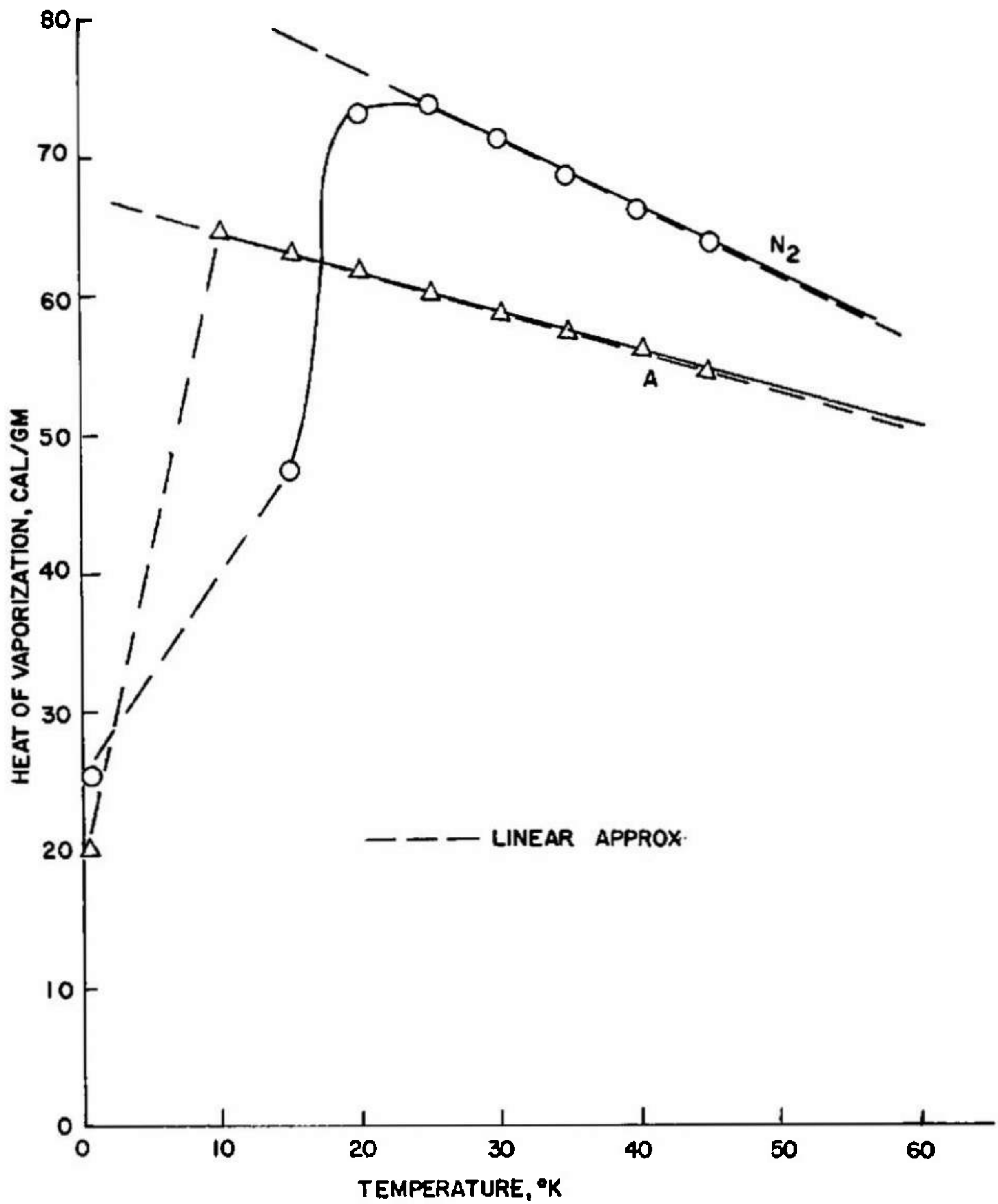

a. Nitrogen and Argon

Fig. 24 Heat of Vaporization

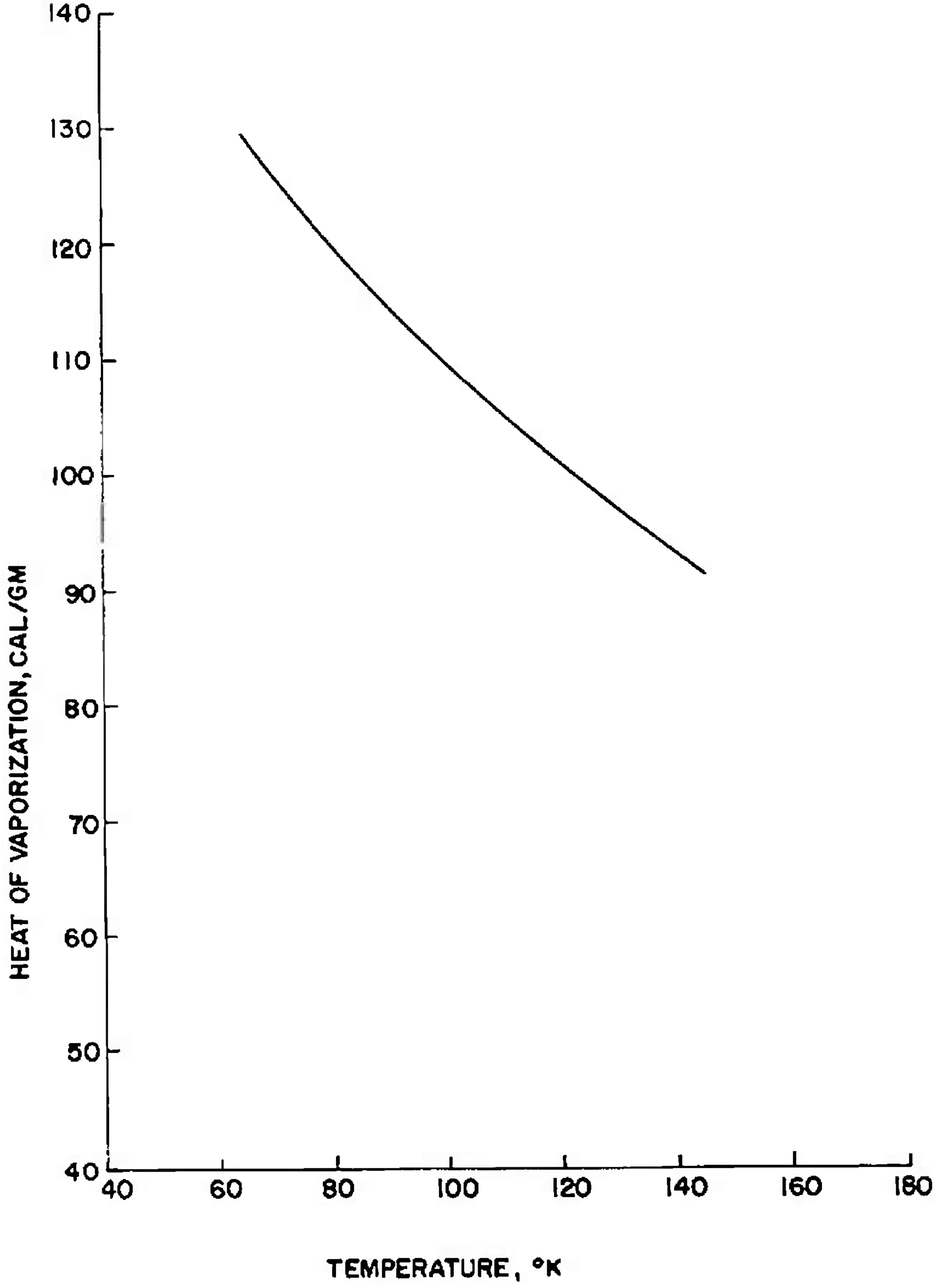

b. Carbon Dioxide

Fig. 24 Concluded

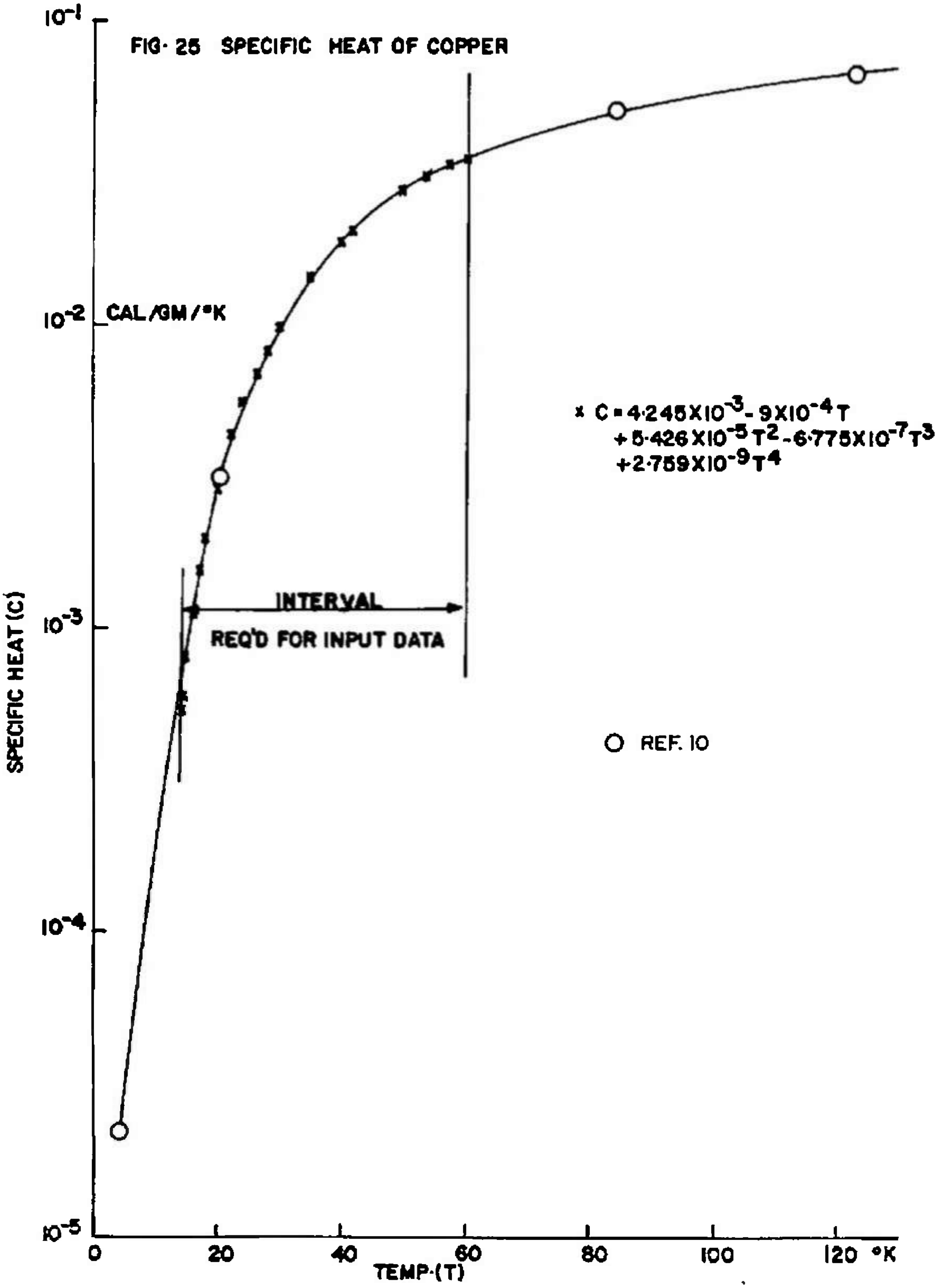

Fig. 25 Specific Heat of Copper

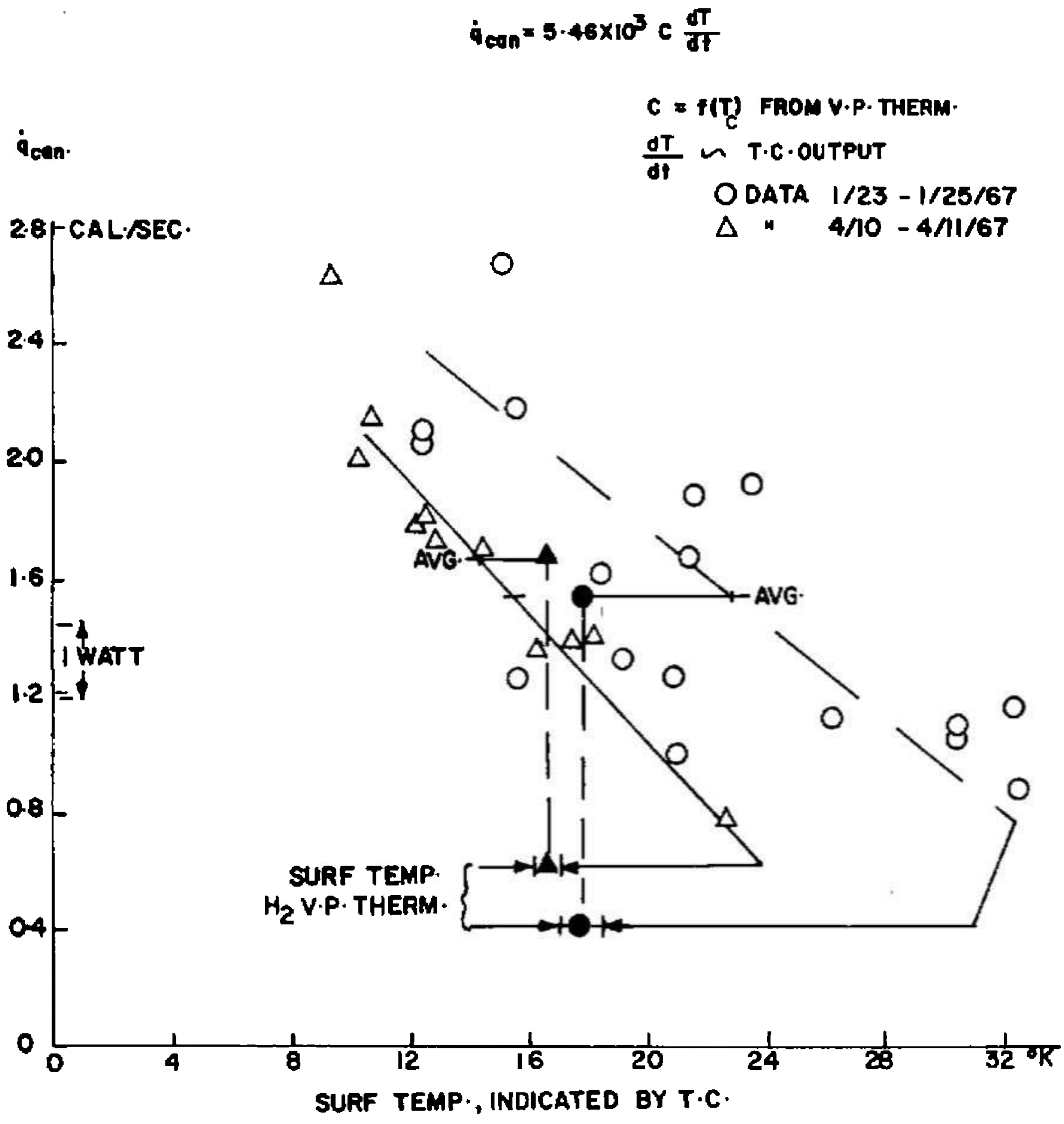

Fig. 26 Apparent Heat-Transfer Rate to Cryosurface in Canister

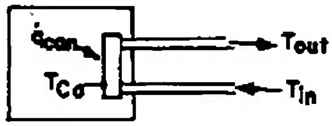

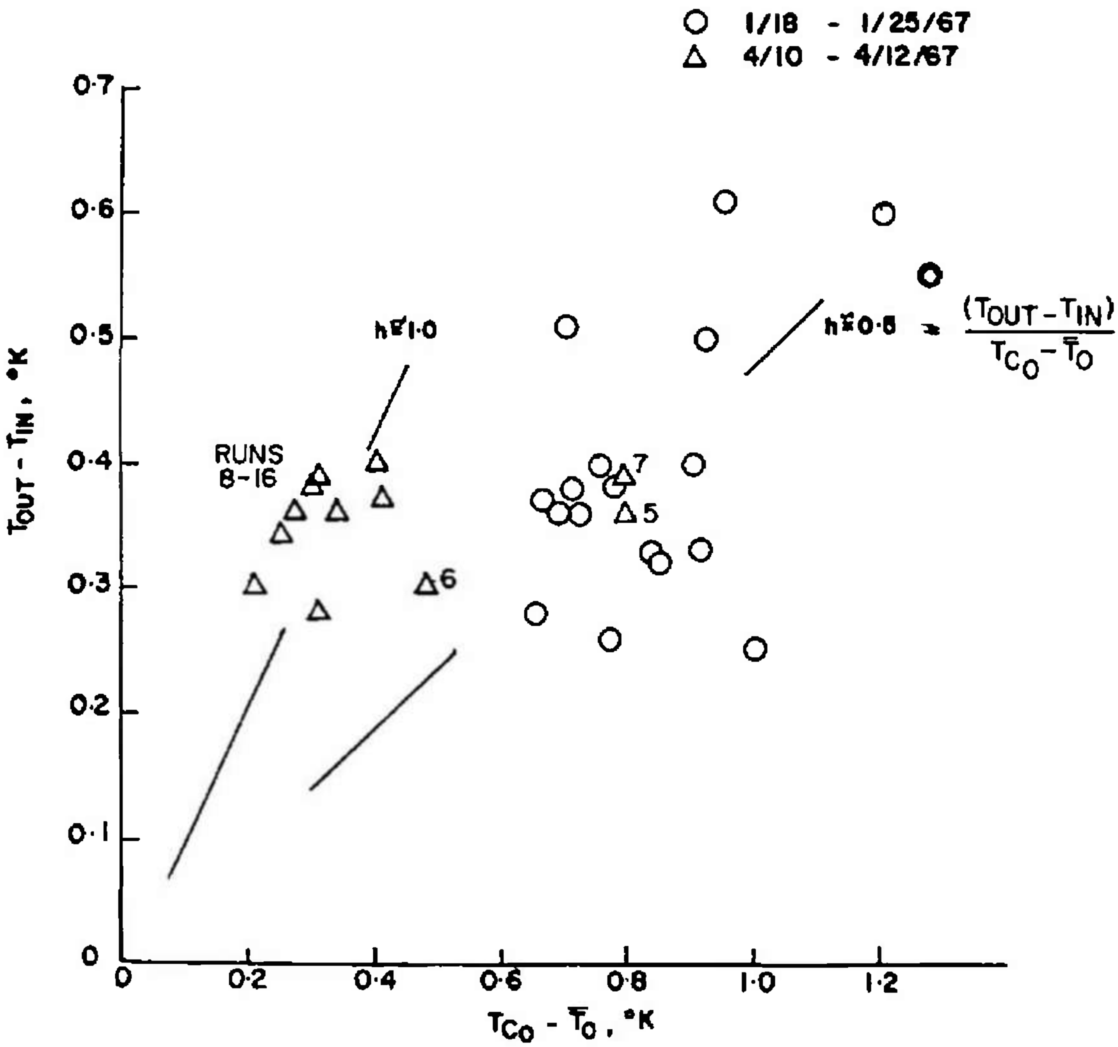

Fig. 27 Steady-State Temperature Differences

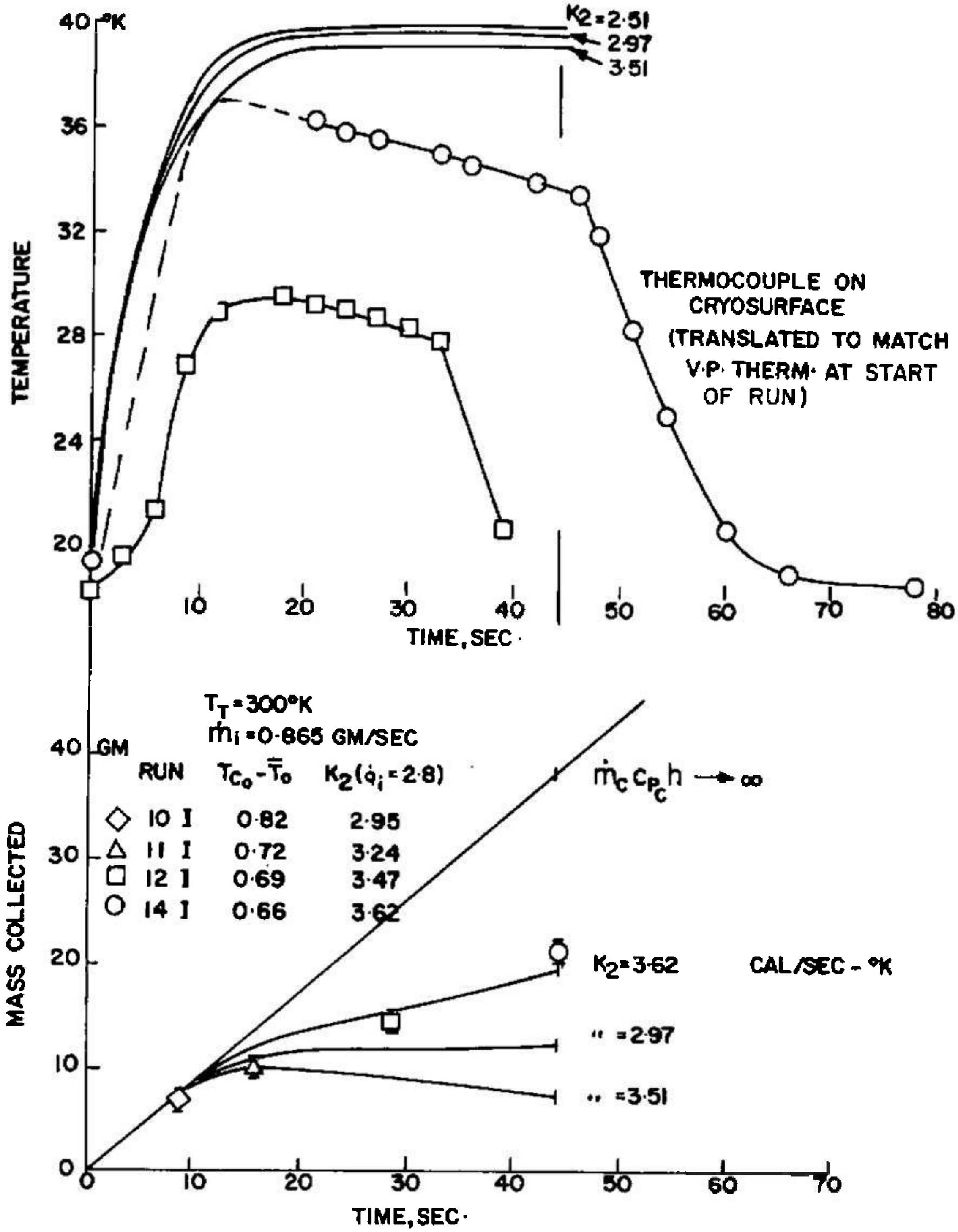

Fig. 28 Effect of Cooling Parameter on Calcuated Gas Collected

$$K_2 = \dot{m}_i C_{p_i} + \dot{m}_c C_{p_c}\left(\frac{2}{2 + h}\right)$$

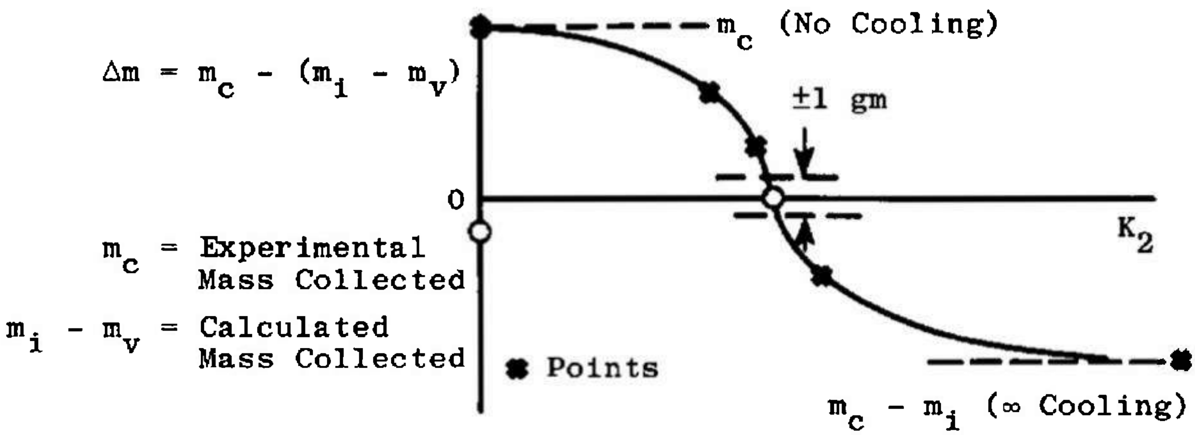

Fig. 29 Difference of Observed and Calculated Collected Mass

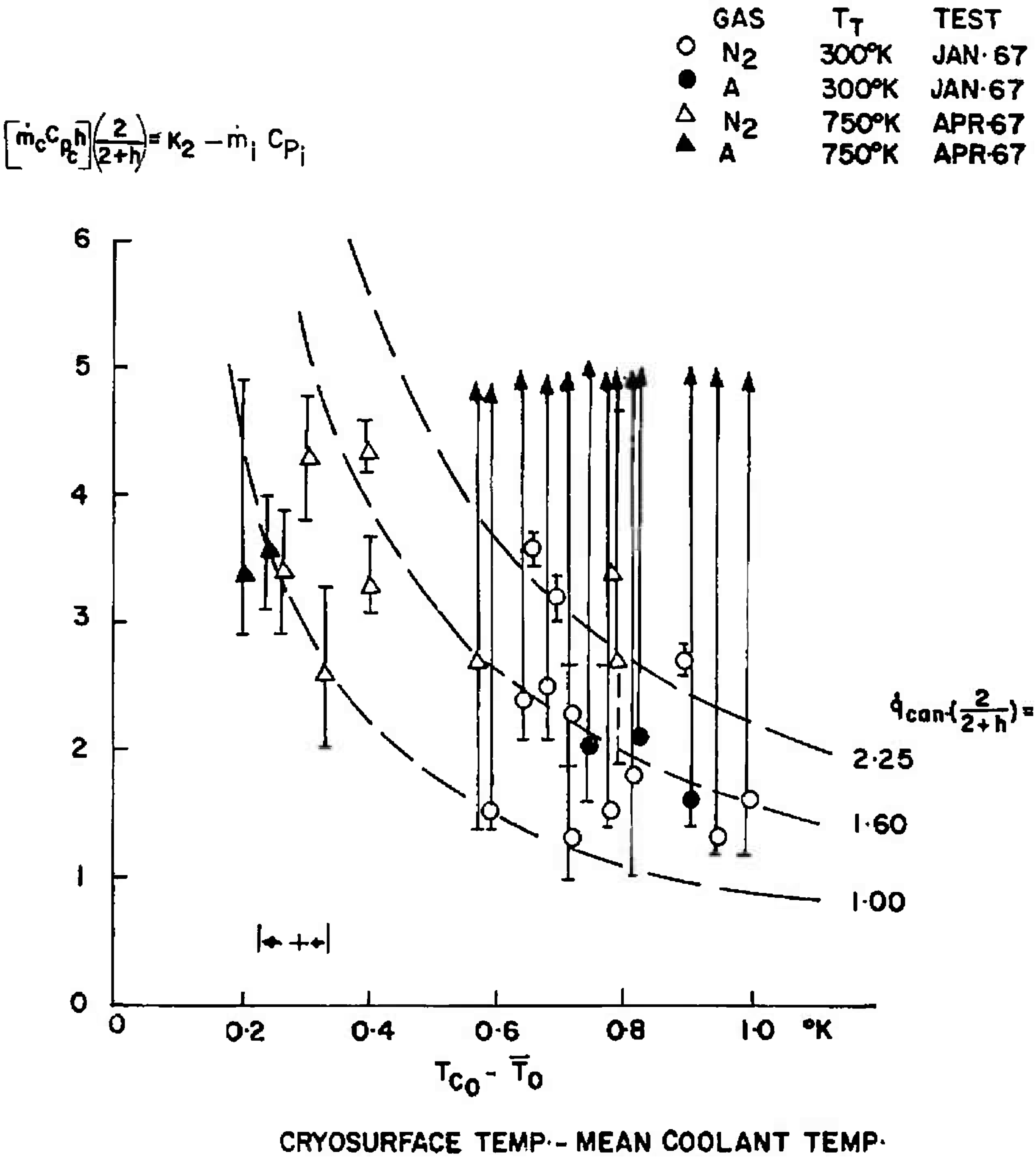

Fig. 30 Cryogenic Cooling Parameter Deduced by Comparing Calculated and Measured Mass Collected

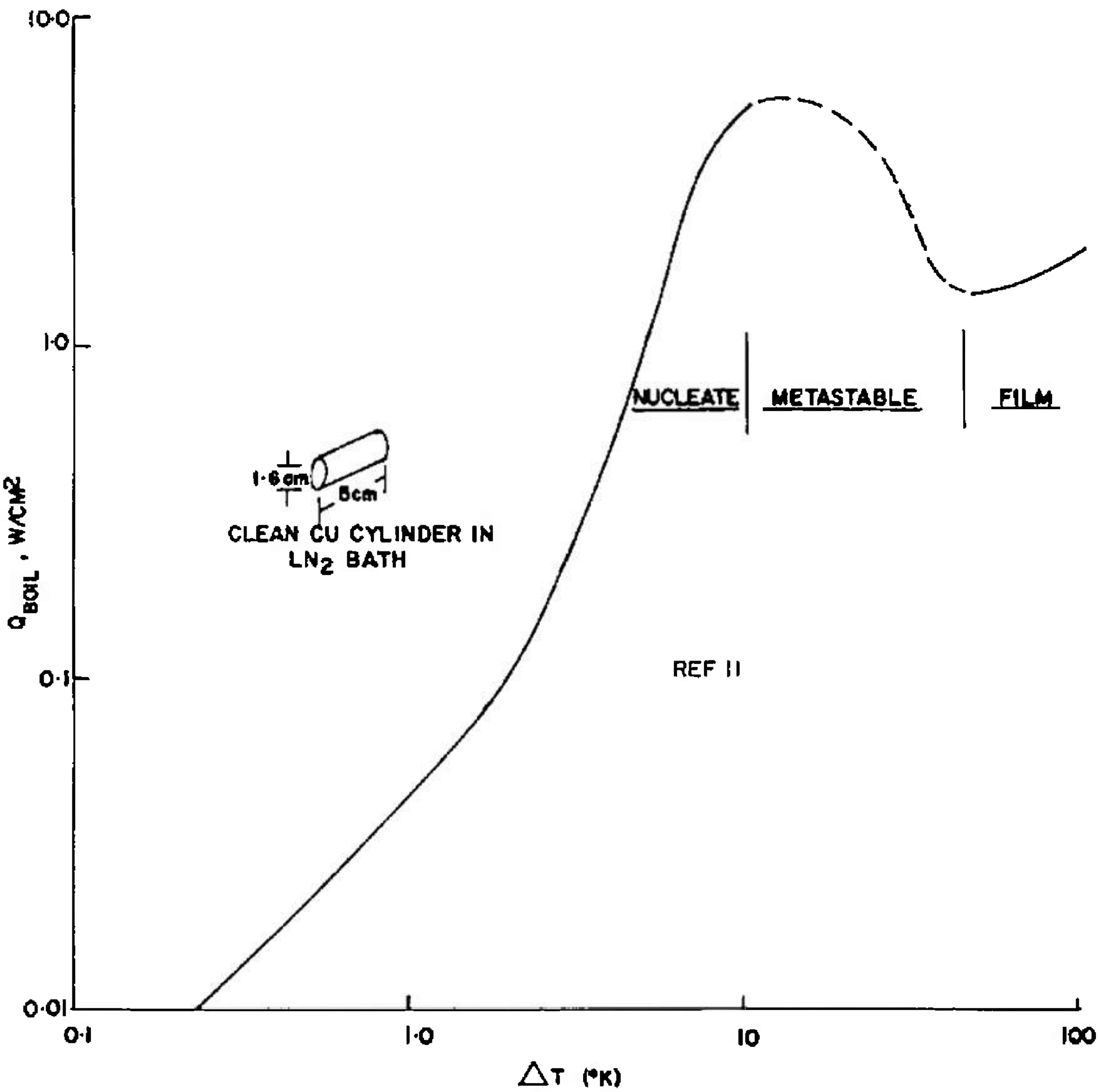

Fig. 31 Boiling Heat Transfer of Liquid Nitrogen

APPENDIX II
CORRELATION OF SHOCK DETACHMENT DISTANCE WITH CONDENSATION FRACTION

During the experimentation for Ref. 1, perforated disks the same size as the cryosurface were placed in the nozzle flow in an attempt to find a relation between the bow shock position and the amount of gas condensed. A solid disk and two plates with 36- and 63-percent open area were photographed while the stream flow was made visible by a 10-MHz RF generator. The air stream conditions were: supply pressure of 150 μ Hg and total temperature of 480°K, which results in an incident mass flow of 0.42 gm/sec. When the cryosurface temperature rose to about 36°K a shock wave appeared near the surface. Figure 23 shows an evaporation rate of 0.1 gm/sec at this temperature, which is an appreciable fraction of the incident flux. With a further increase in temperature, the shock approached the solid disk position.

In Ref. 1 there was no attempt to reduce the photographic data beyond the statement ". . . the capture coefficient for the cryosurface must be greater than 63 percent before the normal shock is eliminated." This was based on the observation that there was a shock wave ahead of the 63-percent porosity plate.

Some further analysis of the photographs appeared to be worth the effort, so they were projected and the shock position was traced (see Fig. 15 of Ref. 1). Geometrical corrections for the camera and model positions were applied to produce the shock detachment distance, δ, in terms of the disk diameter, D.

Figure II-1 illustrates the simple inlet model assumed, where

$$A_H = \text{Hole Area}$$

$$A_D = \text{Disk Area}$$

$$\text{Porosity, } \pi = \frac{\Sigma A_H}{A_D}$$

A capture fraction is defined:

$$C = \frac{\dot{m}_H}{\dot{m}_D} = \frac{\rho_2{}^* u_2{}^* \Sigma A_H}{\rho_\infty u_\infty A_D} = \pi \frac{\rho_2{}^* u_2{}^*}{\rho_\infty u_\infty} \qquad \text{(II-1)}$$

the $(\rho_2{}^* u_2{}^*)$ term is the mass flow through a sonic orifice from stagnation conditions behind a normal shock wave. The ρ_∞ and u_∞ are the density and velocity in the undisturbed stream. By the manipulation of

the adiabatic perfect gas formulas the capture ratio can be written as a function of stream Mach number and ratio of specific heats

$$\frac{C}{\pi} = \left(\frac{\rho^*}{\rho_{T_1}}\right) \frac{a^*}{a_T} \frac{\left(\rho_{T_2}/\rho_{T_1}\right)_M}{M\left(\frac{a}{a_T}\right)_M \left(\frac{\rho}{\rho_{T_1}}\right)_M} \tag{II-2}$$

The values marked with an asterisk are the sonic point isentropic values of density and acoustic speed, a. The term M is the stream Mach number where the stagnation pressure ratio (P_{T_2}/P_{T_1}) and the isentropic ratios (a/a_T) and (P/P_{T_1}) are evaluated. The term C/π has a value of unity at M = 1. If C is set equal to one in Eq. (II-2), the effective porosity required for the shock detachment distance to approach zero can be computed (Fig. II-2). From Eq. (II-2), the capture fraction can be related to porosity, π. The observed shock detachment distance is empirically a function of porosity as shown in Fig. II-3a. The two relations are combined in Fig. II-3b to correlate the shock position with capture fraction. From Eq. (II-2) the capture ratio is 88 percent for 63-percent porosity and for C = 1, a porosity of 92 percent is required.

Because of the effect of viscosity on the flow through the holes, the actual porosity is less than the geometrical values plotted. The two experimental points should lie to the left by some unknown amount; this would produce a more realistic curve for capture fraction as a function of shock detachment distance.

It seems to be necessary for the net condensation rate to exceed 90 percent in order for the shock wave to be obliterated. This conclusion is consistent with observed ratio of collected to incident masses.

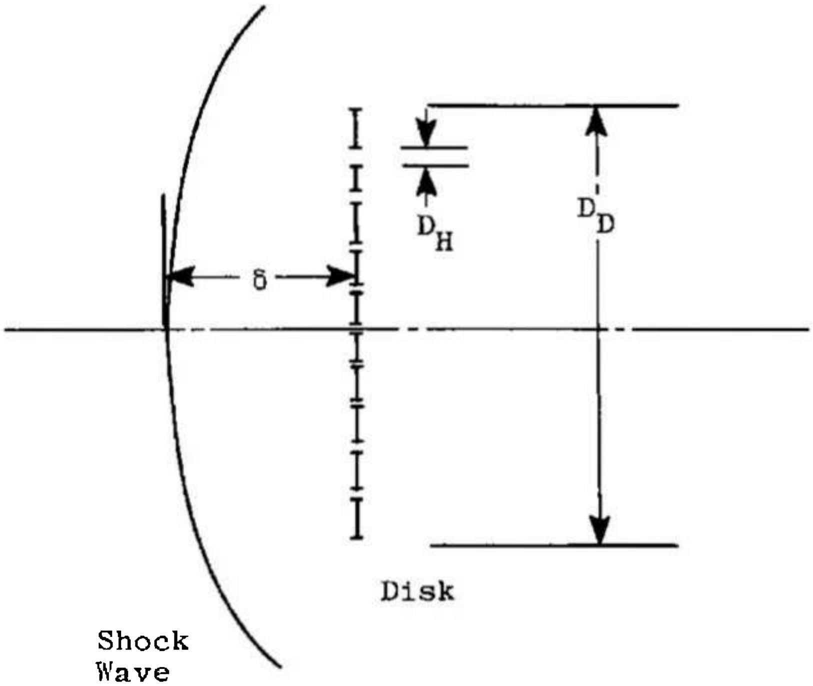

Fig. II-1 Assumed Inlet Model

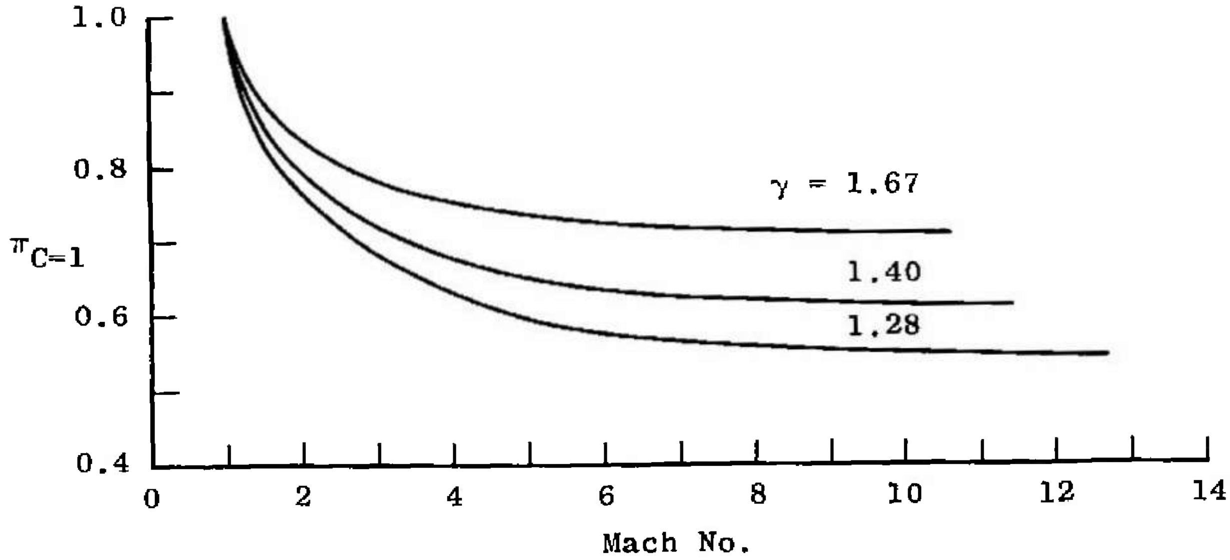

Fig. II-2 Porosity versus Mach Number for C = 1

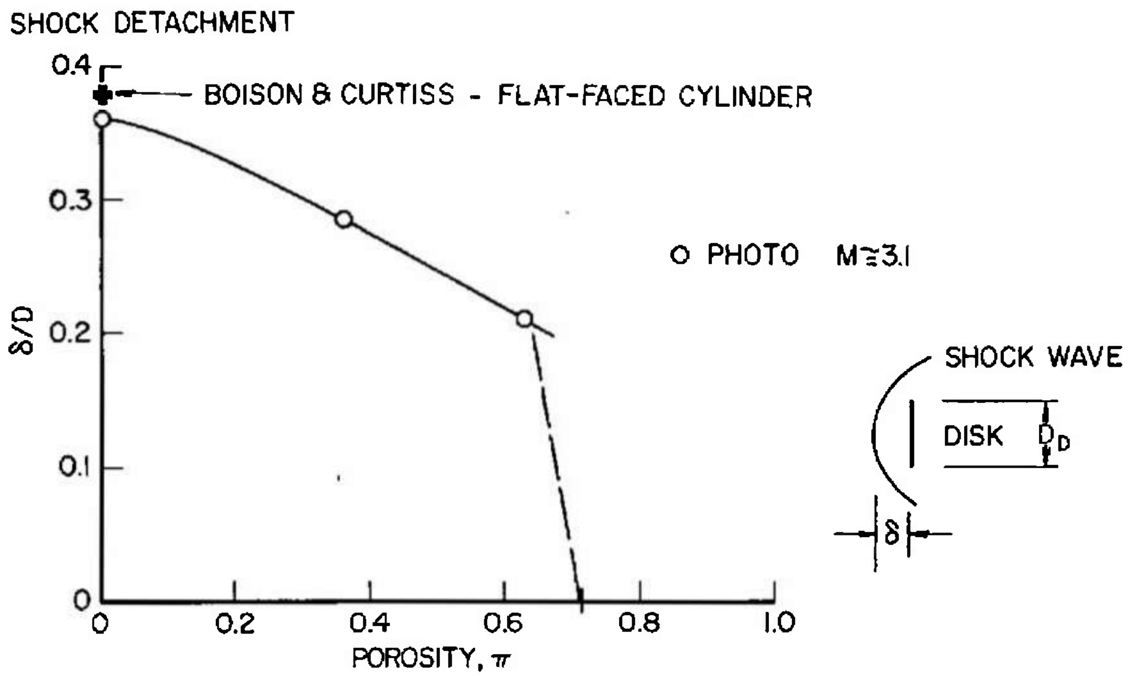

a. Effect of Plate Porosity on Shock Detachment Distance

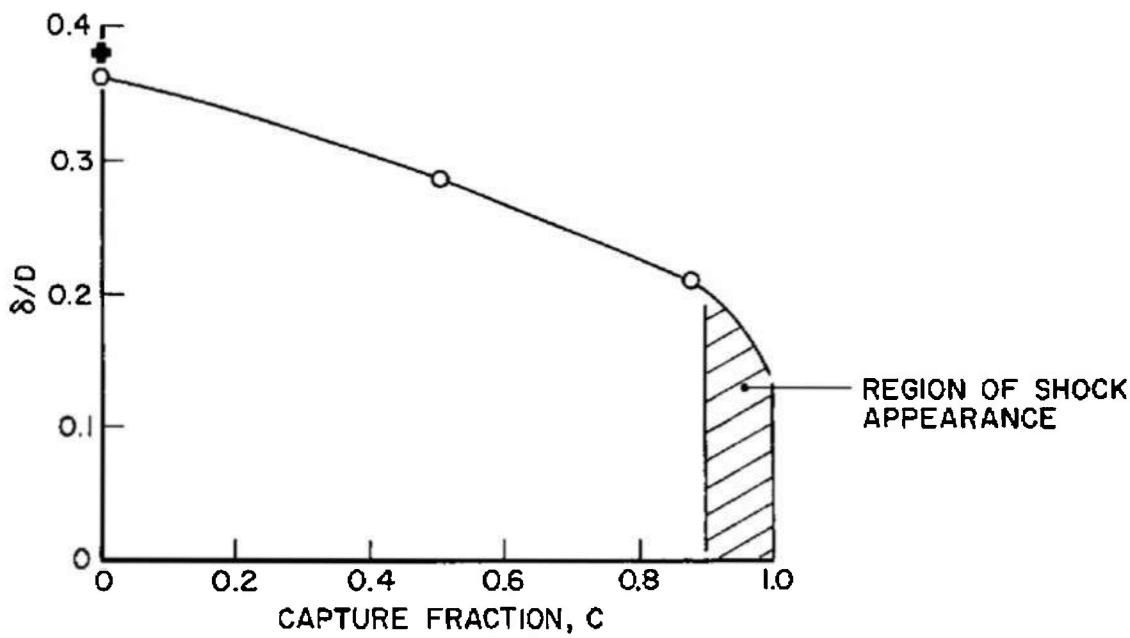

b. Capture Fraction Associated with Porosity

Fig. II-3 Correlation of Bow Shock with Capture Fraction

UNCLASSIFIED

Security Classification

DOCUMENT CONTROL DATA - R & D

(Security classification of title, body of abstract and indexing annotation must be entered when the overall report is classified)

1 ORIGINATING ACTIVITY (Corporate author) Arnold Engineering Development Center ARO, Inc., Operating Contractor Arnold AF Station, Tennessee	2a. REPORT SECURITY CLASSIFICATION UNCLASSIFIED 2b. GROUP N/A

3 REPORT TITLE

THE COLLECTION OF A NORMALLY INCIDENT LOW DENSITY SUPERSONIC STREAM BY A CRYOGENIC SURFACE

4 DESCRIPTIVE NOTES (Type of report and inclusive dates)

January 1965 to June 1967 - Final Report

5 AUTHOR(S) (First name, middle initial, last name)

W. B. Stephenson, ARO, Inc.

6 REPORT DATE	7a. TOTAL NO. OF PAGES	7b. NO. OF REFS
January 1968	71	13

8a. CONTRACT OR GRANT NO AF 40(600)-1200 b. PROJECT NO 8953 c. Program Element 6240533F d. Task 895306	9a. ORIGINATOR'S REPORT NUMBER(S) AEDC-TR-67-201 9b. OTHER REPORT NO(S) (Any other numbers that may be assigned this report) N/A

10 DISTRIBUTION STATEMENT This document has been approved for public release and sale; its distribution is unlimited.

11 SUPPLEMENTARY NOTES	12 SPONSORING MILITARY ACTIVITY
Available in DDC.	Arnold Engineering Development Center (AETS), Air Force Systems Command, Arnold AFS, Tennessee

13 ABSTRACT

An experimental investigation was made to determine the amount of a low density supersonic ($M \cong 3$) gas stream that will condense on a cryogenic surface at normal incidence. Nitrogen and argon flows up to 2×10^{-3} gm/sec/cm^2 at total temperatures from 300 to 750°K condensed on a liquid- or gaseous-helium-cooled plate. The amount collected was related to the stream properties and the heat transfer to the coolant. The analysis indicates that the cryosurface tends to a steady temperature at which the net rate of collection is the incident stream flux minus the evaporation rate for that temperature. This model provides a basis for the design of cryopumping geometries for low density directed flows such as jet plumes or wind tunnel nozzles.

DD FORM 1 NOV 65 1473

UNCLASSIFIED

Security Classification

14 KEY WORDS	LINK A		LINK B		LINK C	
	ROLE	WT	ROLE	WT	ROLE	WT
cryogenics						
supersonic flow						
gas collection						
condensation						